12-2014

Characterization of Biofilms on Medical Device Materials with Application to Reusable Surgical Instruments

Amanda Macaluso
Clemson University, amacalu@g.clemson.edu

CHARACTERIZATION OF BIOFILMS ON MEDICAL DEVICE MATERIALS WITH APPLICATION TO REUSABLE SURGICAL INSTRUMENTS

A Thesis
Presented to
the Graduate School of
Clemson University

In Partial Fulfillment
of the Requirements for the Degree
Master of Science
Bioengineering

---

by
Amanda G. Macaluso
December 2014

Accepted by:
Melinda K. Harman, Ph.D., Committee Chair
Sarah W. Harcum, Ph.D.
Matthew R. Gevaert, Ph.D.

ABSTRACT

Reusable medical devices or reprocessed single-use devices are original medical devices that have been used once and then are cleaned, sterilized, and remanufactured for the purpose of an additional single use on a single patient [4]. Improperly reprocessed devices are a significant contributor to hospital-associated infections [4]. Challenges that hinder reprocessing are related to the complexity of reusable medical device design, the necessary validation of cleaning protocols required by the U.S Food and Drug Administration (FDA), the impact of human factors throughout the reprocessing cycle, as well as economic factors within new business models that are centered on reprocessing.

Current methods for detecting biofilm accumulation on medical devices are established; however, these methods lack appropriate consideration of the complex design features of reusable medical devices. A colorimetric assay widely used for quantifying biofilm accumulation is suitable for the complexity of reusable medical devices; however, its application has been limited to biofilms grown in tissue culture plates, which does not accurately represent the true growth conditions of biofilm. Both material selection and flow conditions are important factors that are known to have an effect on biofilm formation [15, 23]. The broad objective of this thesis was to deliver a simple, cost-efficient method suitable for detecting biofilms on complex reusable medical devices in a high-throughput, industry setting for the purpose of validating cleaning methods required for reprocessing. Specifically, this thesis aimed 1) to grow biofilms under static and dynamic conditions, 2) to develop methods to quantitatively assess biofilm accumulation using a colorimetric assay and confocal laser scanning microscopy

(CLSM), and 3) to apply these methods on commonly used medical device materials with application to reusable surgical instruments.

Successful completion of these aims demonstrated a modified colorimetric assay using crystal violet stain is a highly sensitivity assay that can detect very low concentrations of crystal violet eluted from adhered biofilm. The high sensitivity of this colorimetric assay makes it ideal for detecting biofilm on reusable medical devices with complex design features fabricated from various materials. Additionally, it was shown that CLSM, in combination with image processing techniques, could yield quantitative data for detecting biofilm accumulation by measuring pixilation intensities of biofilm with fluorescent staining. Comparing intensity ratios and absorbance measurements from the colorimetric assay for a given biofilm could demonstrate a direct relationship between the two detection modalities effectively validating the modified colorimetric assay as a method for detecting biofilm accumulation on reusable medical devices. This correlation would be addressed in future work.

The modified colorimetric assay presented in this thesis is a highly sensitive assay for detecting biofilm accumulation. In this regard, it has potential for improving validation methods for cleaning processes required by the FDA for reprocessing reusable medical devices. Moreover, its simplicity and high-throughput potential makes it suitable for industry applications as it relates to human and economic factors. Ultimately, this research work presents a modified colorimetric assay that offers an innovative solution to many of the current challenges associated with medical device reprocessing.

DEDICATION

I dedicate this thesis first and foremost to all of my mentors, past, present and future, who have fostered my pursuits in attaining a high level of academic achievement. Secondly, I dedicate this thesis to my parents for their unwavering support. Lastly, I dedicate this thesis to all who are impassioned by the world of scientific research, wherein, at our very best we are wide-eyed and undeterred by the unsolvables and, wherein, at our very worst we become more inspired by what we cannot seem to solve.

ACKNOWLEDGMENTS

I would like to first acknowledge my research advisor, Dr. Melinda Harman, for her guidance, her dedication, and her unwavering commitment to this research and my growth and development as an engineer. To my committee, thank you for your support and your unique perspectives that each of you brought to this work: Dr. Sarah Harcum, specifically, for your expertise in microbiology, fluid dynamics, and data analysis and Dr. Matthew Gevaert, specifically for your commercial influence, ‘big picture’ perspective, and mentorship. I would also like to thank Dr. Terri Bruce and Rhonda Powell at the Clemson Light Imaging Facility for their vast knowledge in microscopy that contributed significantly to this work. Finally, I would like to thank all members of the ReMed Laboratory and the entire Department of Bioengineering at Clemson University, without whom I would not have been able to complete this work.

TABLE OF CONTENTS

Page

Table of Contents (Continued)..... Page

LIST OF TABLES

LIST OF FIGURES

CHAPTER ONE

INTRODUCTION

1.1 THE GLOBAL MEDICAL DEVICE REPROCESSING MARKET

The global medical device reprocessing market is currently (2014) estimated at $780 million U.S. dollars (USD) and is expected to grow at a compound annual growth rate of 19.3% to become a $2.6 billion USD industry by 2020 [1]. This market is one of the fastest growing markets in healthcare today because of three key factors that are driving its growth. The first is the demand for reusability to cut healthcare spending. In the healthcare industry today the revenue model for providers is no longer based on throughput alone. As a result, there is a shift towards value-based care in which providers can maintain high levels of care without increasing the cost of care. Reusability of devices is a value-based care model. The 3,000 U.S. hospitals that are already using reprocessed devices see a total savings of $336 million dollars yearly [2]. But, if just 2% of single-use devices were reprocessed the healthcare industry would save $2 billion USD each year [2]. The second factor that is driving growth is favorable economic opportunity. The lower price point of reprocessed devices compared to original devices enables device manufacturers to enter new markets, specifically, the global healthcare market [3]. In this regard, reprocessing increases economic opportunity for many original device manufacturers. The third factor that is driving growth is environmental sustainability. In addition to saving costs, reprocessing is also eliminating waste. The healthcare industry is the second largest contributor to landfills in the U.S., generating over 4 billion pounds of waste annually [2]. Reprocessing can help hospitals eliminate

approximately 9 million pounds of waste each year [1]. The sustainability of reprocessing further drives the momentum of this industry.

While the medical device reprocessing industry is thriving economically, it is not without shortcomings. Improperly reprocessed devices are a significant contributor to hospital-associated infections [4]. This chapter will provide an overview of how medical device reprocessing works and the microbiological and engineering factors that can create challenges for reprocessing.

1.2 A SYSTEMATIC PROCESS

Medical device reprocessing is a highly regulated, systematic process. In general, though, it can be simplified into six distinct phases: collection, inspection, cleaning, remanufacturing, sterilizing, and distribution. 1) The process begins with collection at the point-of-use of the device in the operating room or clinic. 2) Used devices are properly disposed in a designated storage container and later collected and transported to either an on-site or off-site reprocessing facility. The inspection phase involves visual assessment for gross damage. Devices beyond repair are discarded. 3) There the devices that pass visual inspection are disassembled for cleaning. A combination of chemical and physical processes is required to remove all visible bioburden. 4) The remanufacturing phase involves reassembly of the cleaned devices, remanufacturing, and functional testing. Many reprocessed devices have sharp blades that may need to be re-sharpened or disposable components that need to be replaced. After reassembly and remanufacturing the device is tested for function and performance. 5) If the device meets the function and

performance specifications, it is then either disinfected or sterilized in accordance with FDA requirements. This choice is dependent upon the degree of risk of infection determined by the Spaulding classification system, in which reprocessed devices are classified as either critical, intended for contacting sterile body tissues or cavities; semi-critical, only intended to contact mucous membranes and is not intended to penetrate sterile body tissues or cavities; or non-critical, intended for topical contact only [5]. Non-critical devices require low-level disinfection, semi-critical devices require high-level disinfection, and critical devices require sterilization. 6) After the device has been disinfected or sterilized, it is repackaged and relabeled for distribution.

1.3 COMPLEXITY IN RESUABLE MEDICAL DEVICE DESIGNS

Reusable medical devices or reprocessed single-use devices are original medical devices that have been used once and then are cleaned, sterilized, and remanufactured for the purpose of an additional single use on a single patient [4]. Reusable medical devices encompass a wide variety of invasive surgical instruments that are used in cardiovascular, orthopedic, and general surgical procedures. There are also many non-invasive devices, such as pneumatic tourniquet cuffs and pulse oximeter sensors that are reprocessed. Though there are a wide variety of reusable medical devices many of these devices have similar modes of action and, subsequently, have similar design features. **Table 1.1** provides a broad list of reusable medical devices and key design features. The design features commonly associated with these devices are complex, which creates significant challenges in cleaning. Some examples include, long and narrow lumens that are

impossible to fully visualize and confirm complete removal of bioburden, intricate cutting teeth and apertures that are difficult to brush, and non-modular components that are simply inaccessible for manual cleaning and inspection. Also, many of these devices have optics and electrical components that must be considered in both cleaning and sterilization techniques, as these components cannot be immersed in cleaning or disinfection solutions. In addition to creating difficulties in cleaning and sterilization, complex design features provide increased opportunity for biofilm accumulation. Biofilm accumulation in reusable medical devices is the primary risk factor for infection.

Table 1.1: Commonly reprocessed reusable medical devices and key design features. Reusable medical devices are diverse, but share similar design features that are challenging for cleaning.

Reusable Medical Device	Key Design Features
Arthroscopic Shaver	narrow,long lumens; flexible tubing; electrical; ergonomic hand piece; blades and burs
Biopsy Forcep	narrow, long lumens; blades; angulated and straight jaws
Endoscope	narrow,long lumens; flexible tubing; optics; electrical; ergonomic hand piece
External Fixation Device	modular components (i.e nuts and bolts); intricate aperatures
Tourniquet	flexible tubing; velcro cuff
Trocar	narrow lumens; modular components (i.e removable sheaths); blades
Vessel Sealer	narrow, long lumen; ergonomic hand piece; electrical; angulated and straight jaws

1.4 BIOFILMS: A CHALLENGE FOR CLEANING AND STERILIZATION

Potential infection from reprocessed devices is a major concern because of unique microbial populations known as biofilms. Biofilms are a diverse, dynamic, and adhered microbial population retained within a secreted extracellular polysaccharide (EPS) matrix [6]. There are four key physiological characteristics that differentiate biofilms from planktonic or free-floating bacteria. 1) A heterogeneous population of microbial organisms within a supporting EPS matrix that provides a three-dimensional hydrated structure for the biofilm that can vary in space and time. 2) A differing genetic expression from planktonic bacteria makes biofilms impervious to targeted pharmacological therapies that have already been established for non-biofilm bacteria. 3) A highly developed and coordinated intercellular signaling mechanism, termed quorum sensing, enables biofilms to have a controlled, dynamic response to the environment. As a result, biofilm structure and composition varies widely. 4) A dramatic reduction in susceptibility to antibiotics and antimicrobials makes biofilms 1000X more resistant than non-biofilm bacteria [6]. Biofilms are protected within in a three-dimensional structure limiting the penetration of antimicrobials. Additionally, cells deep within the EPS show reduced metabolic activity as a defense mechanism to chemical agents. Overall, the unique physiological adaptions of biofilms make them extremely resilient to removal.

While biofilms are diverse microbial populations, there are certain pathogens that are more commonly associated with contaminated surgical instruments. Frequently associated with reusable medical devices are *Staphylococcus aureus* (gram-positive), Coagulase-negative *Staphylococci* (CoNS) (gram-positive), and, *Pseudomonas*

aeruginosa (gram-negative) [7,8]. CoNS are specifically common to reusable surgical instruments because these bacteria are normal inhabitants of the skin and mucous membranes [9]. CoNS are opportunistic pathogens that have a propensity to form biofilms. The most prevalent species of CoNS, accounting for approximately 60-70% of all CoNS on the skin, is *Staphylococcus epidermidis* [9].

Biofilm accumulation on reusable medical devices poses a high risk for infection; however, the process of biofilm formation can be mitigated if cleaning and sterilization occur promptly after use (**Table 1.2**). Biofilm formation occurs in a gradual process [10]. First, reversibly attached microcolonies begin to form where there is a conditioning layer. For reusable medical devices this may be urine, blood or some other protenaceous substance. Colonizing bacteria then begin to form initial attachments to the preconditioned surface. At this point, the biofilm is not fully attached and can easily be removed by cleaning. However, if it is not cleaned immediately then irreversible attachments will ensue through the production of EPS. The emerging microbial community will continue to grow and develop until it cannot sustain itself. The biofilm can then propagate through detachment and dispersal allowing it to reattach to nearby surfaces and maintain its viability. Recognizing the potential risk for infection if devices are not properly cleaned and sterilized immediately after use, the U.S Food and Drug Administration (FDA) has increased regulatory requirements and provided detailed guidance documents to ensure reprocessed devices are safe and effective.

Table 1.2: Conditions required for biofilm formation (adapted from Roberts, C.G. 2013) [19]. This table lists the necessary conditions required for biofilm formation. Reusable medical devices provide the conditions necessary for biofilm formation; however, irreversible attachment can be prevented if reprocessing steps occur immediately after use because the time required for development of a biofilm can be controlled.

Condition	Potable Water Pipe	Indwelling Medical Device	Reusable Medical Device
Colonizing microorganism present	yes	yes	yes
Surface to be colonized	yes	yes	yes
Sufficient nutrients and water	yes	yes	yes
Necessary temperature conditions for growth	yes	yes	yes
Time required for biofilm development	yes	yes	?

1.5 CONSIDERATIONS FOR IMPROVING MEDICAL DEVICE REPROCESSING

In 2002 the FDA enacted the Medical Device User Fee and Modernization Act (MDFUMA), which required manufacturers of reprocessed devices to submit validation data for cleaning, sterilization and functional performance [12]. Every reprocessing provider must adhere to the standards set forth by the original device manufacturer (OEM) and prove each device can be adequately reprocessed and meet the standards for function and performance. Additionally, MDFUMA requires OEMs to provide proper labeling and comprehensive Instructions For Use (IFU) documents to detail the reprocessing procedures approved for each specific reusable device. Despite this high degree of regulation, the literature reports many reprocessed devices still fail to meet reprocessing standards for safety and performance [7,8,11]. For this reason, verification and validation of the cleaning, disinfection, and sterilization processes required in reprocessing has been a point of discontentment for both OEMs and reprocessing service providers in the healthcare industry.

During the 2011 Medical Device Reprocessing Summit hosted by The Association for Advancement in Medical Instrumentation (AAMI) and the FDA, the number one call to action focused on improving adequate cleaning validation protocols for reprocessing reusable devices [13]. Moreover, in 2011 the FDA also published guidelines recommending that human factors be considered in reprocessing validation, as human factors are critical for maintaining reproducibility and repeatability of adequately reprocessed devices in a high-volume throughput [14]. In order to improve medical device reprocessing there are three key factors to be considered: 1) a better definition for

how “clean” is clean; 2) reusable medical device designs that consider reprocessing from the very early stages of device development; and 3) human factors related to reprocessing protocols [13]. In addition to these three considerations, there is a fourth indirect consideration for improving reprocessing: cost. The economic model of reprocessing is not a favorable one for OEMs. Reduction in purchase of new products results in a reduction of revenue for the OEM. Consequently, OEMs are neither incentivized to design their devices for reprocessing nor are they incentivize to produce feasible reprocessing protocols that can be adequately executed in an industrial system. Therefore, reducing costs associated with reprocessing for the OEM is another consideration for improving medical device reprocessing outcomes.

1.6 PURPOSE

The demand for reusability and the favorable economic environment have driven rapid growth in the global medical device reprocessing market. Consequently, industry leaders have recognized key challenges for reprocessing from both clinical and engineering perspectives that if improved upon could further grow the medical device reprocessing industry and yield better reprocessing outcomes. The principle industry needs are: 1) improved cleaning validation methods; 2) devices that are designed for reprocessing from the very beginning; and 3) reprocessing methods that consider human factors and quality control. The broad objective of this thesis is to deliver a simple, cost-efficient method suitable for detecting biofilms on complex reusable medical devices in a high- throughput, industry setting for the purpose of validating cleaning methods required

for reprocessing. This broad objective will be achieved through three specific aims: 1) to grow biofilms under both static and dynamic flow conditions; 2) to develop methods to quantitatively assess biofilm accumulation using a colorimetric assay and confocal laser scanning microscopy (CLSM); and 3) to apply these methods to commonly used medical device materials with application to reusable surgical instruments (**Figure 1.1**).

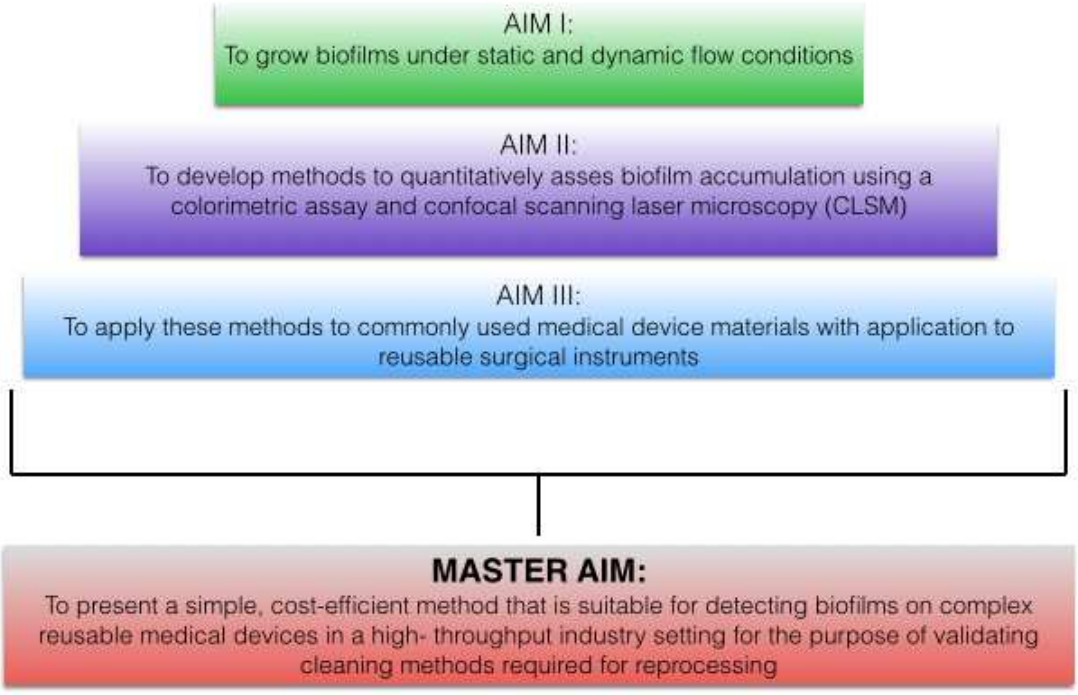

Figure 1.1: Thesis aims and outline. The broad objective of this thesis was achieved through three specific aims; however, these three specific aims were all interdependent, as each focused on developing methods for quantification of biofilm accumulation with application to reusable surgical instruments. In order to maintain structure in this document the thesis aims are discussed in the following manner: Aim I is discussed in Chapter 2; Aim II and Aim III, as related to the colorimetric assay, are discussed in Chapter 2; Aim II and Aim III, as related to CLSM, are discussed in Chapter 3; and the impact of these aims on the Broad Objective is discussed in Chapter 4.

CHAPTER TWO

QUANTIFYING BIOFILM ACCUMULATION ON COMMONLY USED MEDICAL DEVICE MATERIALS

2.1 INTRODUCTION

Quantifying biofilm accumulation on reusable medical devices is necessary for validating cleaning methods required for reprocessing; however, increasing complexity in device design creates challenges for cleaning. [4]. Many design characteristics related to reusable medical devices provide greater opportunities for biofilm growth and accumulation. In addition, these design features can hinder manual-cleaning techniques, such as brushing, and make visual verification of complete removal of bioburden more difficult.

Methods for assessing biofilm on implantable devices for infection-related analyses are already established; however these methods lack appropriate considerations for the complex designs of reusable medical devices. Three principle methodologies include the roll plate method, the endoluminal brush technique, and mechanical removal for fluorescent staining or biochemical testing [15]. The roll plate method, developed by Maki, et al. (1977), assumes bacteria will be recovered by rolling the device onto an agar plate [16]. Recovered organisms are then cultured and quantified through cell counting. The endoluminal brushing technique, developed by Kite, et al. (1997), follows the same premise, but is specific for lumens [17]. Mechanical removal, developed by Donlan, et al. (2001), involves sonication of the device to remove biofilm, which is then homogenized

to produce a biofilm suspension that can be cultured on an agar plate [18]. Colonies could be counted or sub-cultured for fluorescent staining and biochemical testing.

These methods were all developed principally for bacteria recovery on intravenous catheters to determine associated infection and were validated accordingly. However, each of these methods is limited in its applicability to reusable surgical devices. The roll plate method is not suitable to devices with complex features such as lumens or teeth. Moreover, the study by Maki, et al. (1997) reported 90% of the catheters studied had low-density colonization [16]. For this reason, the roll-plate method can distinguish infection, but is not reliable for quantifying biofilm colonization due to a low percentage of recovered organisms [15]. The endoluminal brushing technique is applicable to devices with small diameter lumens; however, it is not feasible for devices with large surface areas. Moreover, the endoluminal brushing technique is not suitable for intricate design features, such as teeth or modular interfaces. Mechanical removal of biofilm using sonication is a widely used method for quantifying biofilm [15, 19] and has proved effective in many cleaning methods [20]; however, this method may not be feasible for devices with assembled, optical, or electrical components. Moreover, this method cannot localize the regions of biofilm accumulation on the reusable medical device. Localization of biofilm accumulation is critical for validating cleaning processes. Recognizing the limitations in current methods, there is a clear need for a quantitative method for detecting biofilm, specifically on reusable devices, for the purpose of validating cleaning methods required for reprocessing.

A colorimetric assay using crystal violet (hereinafter CV) is a standard method for quantifying bacterial adherence for biofilms grown in polystyrene tissue culture plates [21]. The affinity of CV for substances found in the cell walls of bacteria makes CV staining a highly sensitive stain for both live and dead cells when compared to the previously discussed methods [17]. When used in combination with a decolorizing agent that breaks down the lipid structures, the membrane is permeabilized, allowing the release of CV complexes from the cell walls (**Figure 2.1**). The released CV can then be quantified to determine the amount of adhered biofilm. By measuring the absorbance of the released CV a direct relationship between absorbance and bacteria concentration can be determined [21]. In this regard, this colorimetric assay is a quantitative method for detecting biofilm adherence to tissue culture plates.

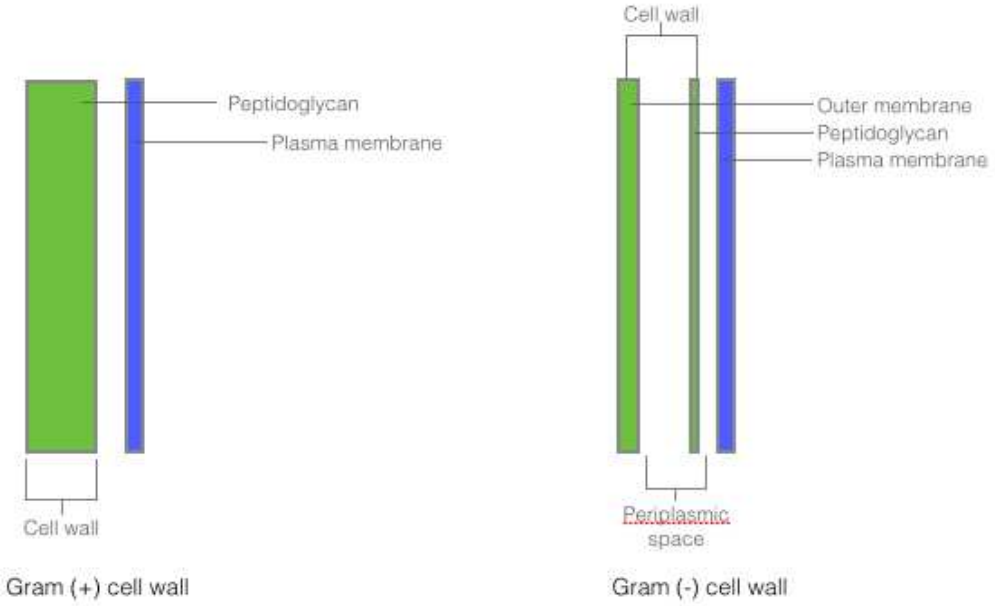

Figure 2.1: Schematic of bacteria cell wall structures (adapted from Rudolph, K. 2012) [22]. CV preferentially binds to peptidoglycan in bacteria cell walls, making it a unique stain for detecting bacteria. Gram-positive bacteria have cell walls that are comprised of approximately 90% peptidoglycan with a thin outer membrane. The outer membranes of bacteria cell walls are characterized by high lipid- content, which can be permeabilized by decolorizing agents, such as acetic acid.

While the current recovery methods for detecting biofilm accumulation are well established, these methods lack appropriate considerations for the complex design features of reusable medical devices (**Table 2.1**). A colorimetric assay is more suitable for complex designs. Additionally, a colorimetric assay is a highly sensitive method for biofilm detection and can localize biofilm accumulation. However, established colorimetric assays only assess biofilms grown in a tissue culture plate, which does not accurately represent the true growth conditions of biofilm. Both material selection and flow conditions are important factors that are known to have an effect on biofilm formation [15, 23]. These parameters will vary for reusable surgical instruments; therefore, material selection and flow conditions must be considered in developing methods for detecting and quantifying biofilm accumulation specifically for reusable devices. The present study will implement a modified [23] ASTM method (ASTM 2647-08) for growing *Stapylococcus epidermidis* biofilms under dynamic flow conditions in a drip flow reactor. The purpose of this study was to mimic relevant biofilm growth conditions and modify a colorimetric assay for quantifying biofilm accumulation. First, biofilms were grown under both static and dynamic conditions on coupons representative of four commonly used medical device materials: 316L stainless steel, polycarbonate, polypropylene, and silicone rubber. Second, an existing colorimetric assay [21] was modified to appropriately stain biofilm grown on large surface areas.

Table 2.1: Comparison of methods for detecting biofilm on complex reusable medical devices. Four methods (discussed above) were compared for suitability in detecting biofilm on complex design features of reusable medical devices. In comparison to current methods, the CV assay is suitable for detecting biofilms on the most design features, while also providing high sensitivity of detection and localization of biofilm growth.

Design Feature of Reusable Medical Devices	Roll Plate Method	Endoluminal Brush Technique	Mechanical Removal Method	CV Assay
long, narrow lumens	no	yes	yes	yes
modular interfaces[1]	no	no	yes	yes
blades/jaws[2]	no	no	yes	yes
optical devices[3]	yes	yes	no	no
electrical devices[4]	yes	yes	no	no
large, assembled[5] components	yes	yes	no	yes
Degree of Sensitivity	low	low	high	high
Localization of Biofilm Growth	no	yes	no	yes

[1]modular interfaces refers to the presence of crevices
[2]blades/jaws refers to small teeth <1 mm in lateral distance
[3]optical devices refers to any device with camera or lens
[4]electrical devices refers to any device requiring power to operate
[5] assembled components refers to components that can not be disassembled

2.2 MATERIALS AND METHODS

Bacterial species/strains and culture preparation

Staphylococcus epidermidis ATCC 12228 stock cultures were streaked on Tryptic Soy Agar (TSA) plates and incubated overnight at 37°C to obtain isolated colonies. A single colony was transferred to 30 g/L Tryptic Soy Broth (TSB) media and grown overnight in a shaker incubator at 37°C and 125 rpm to either a high (9.68± 0.4 Log_{10} CFU/mL) or a low (5.35±0.07 Log_{10} CFU/mL) inoculum concentration. The overnight cultures were used to inoculate the experimental coupons. Stock cultures were frozen in 1:1 of 20% sterile glycerol and media. Bacteria were recovered in 10 mL of media and incubated for 24 h at 37°C.

Coupons and cleaning procedure

Biofilms were grown on 25 x 75 x 1mm coupons, comparable in size to a standard glass microscope slide. Coupons were manufactured (Model No. DFR-2575, Biosurface Technologies, Bozeman, MT) from materials relevant to reusable medical devices: 316L stainless steel, polycarbonate, polypropylene, and silicone rubber.

Prior to use, coupons were cleaned and sterilized. Individual coupons were soaked in a 1% enzymatic detergent for 20 minutes, removed and gently cleaned with nylon brush for 30 seconds on each side. Coupons were rinsed in tap water and followed by sonication (Brunson 5510, Branson Ultrasonics Corporation, Danbury, CT) in tap water for 10 minutes to mechanically remove visible bioburden. Following sonication, coupons were rinsed with filter-sterilized water (Milli-Q® Integral Purification System, EMD

Millipore, Billerica, MA) to remove any residual detergent. Sonication was repeated in filter-sterilized water for 10 minutes. Coupons were steam sterilized for 20 min at 121°C. Coupons with any visual evidence of surface damage or defects were discarded.

Dynamic biofilm growth method in drip flow biofilm reactor

Biofilms were grown under dynamic conditions in a drip flow reactor (Model No. DFR 110-4, Biosurface Technologies, Bozeman, MT) according to a standard method (ASTM 2647-08) previously modified for use with staphylococci by Buckingham-Meyer, et al. 2007 [23]. The reactor is designed to accommodate four coupons in compartmentalized channels, each with its own influent and effluent ports (**Appendix B.1**). Design of experiment was determined by the constraints of the four channels, which is described in **Table 2.1**. Sterile coupons of each material were placed in the appropriate channels. Each channel, containing 15 mL of 30 g/L TSB, was inoculated with 1 mL of the *S. epidermidis* inoculum at either a high (9.68± 0.4 Log_{10} CFU/mL) or a low (5.35±0.07 Log_{10} CFU/mL) inoculum concentration. Biofilms were initially grown in an incubator in batch conditions at a 0° position for 6 h at 37°C. Continuous flow was initiated by placing the reactor on a stand oriented at a 10° angle and pumping 3 g/L TSB at a flow rate of 0.92 mL/min/channel using a peristaltic pump system (Model No.7553-80, Cole-Palmer) with four pump heads (Model No. 7518-00, Cole-Palmer) (**Appendix B.2**). The rate of flow yields a "drip" effect through the influent valve. The orientation of the reactor allows gravitational force to produce a low shear fluid flow over the growing biofilm. Biofilms were grown in continuous flow conditions in an incubator at 37°C for 48 hrs.

Static biofilm growth method

Biofilms were grown under static conditions in sterile petri dishes. Sterile coupons of each material were placed in sterile petri dishes, each containing 15 mL of 30 g/L TSB, and inoculated with 1mL of *S. epidermidis* inoculum at either a high (9.68± 0.4 Log_{10} CFU/mL) or a low (5.35±0.07 Log_{10} CFU/mL) inoculum concentration and grown in an incubator at 37°C for 54 hrs.

Experimental design

The modified colorimetric assay was implemented for each material under each growth condition. Dynamic and static biofilm growth methods were run in parallel yielding a total of eight coupons per experiment. The four-channel capacity of the drip flow reactor determined the experimental design. In order to minimize inoculum variation and potential channel bias, all four material types were used in each experimental run and each material type was run in each position of the drip flow reactor at least once. **Table 2.2** shows the rotation of each material type through each channel of the drip flow reactor**.** In addition to the variables, material and flow condition, acetic acid volume and excitation wavelength were also assessed (**Table 2.3**). Five replicates of each coupon type were grown under both dynamic and static conditions, eluted using 20 mL of acetic acid and examined at an excitation wavelength of 492 nm. Two of these replicates were also examined at an excitation wavelength of 570 nm. Two replicates of each coupon type were grown under both static and dynamic conditions, eluted using 6 mL of acetic

acid and examined at excitation wavelengths, 492 nm and 570 nm. In this manner, a total of seven replicates of each coupon type were examined.

Table 2.2: Experimental design for testing of four selected materials in drip flow reactor. This design tests all four material types during each experimental run and rotates materials through each channel of the drip flow reactor (SS= 316L stainless steel, PC= polycarbonate, PP= polypropylene, SI= silicone rubber). Seven replicates for each material type were examined.

	Channel			
Run	1	2	3	4
1	PP	PC	SS	SI
2	PC	SS	SI	PP
3	SI	PP	PC	SS
4	SS	SI	PP	PC
5	PP	PC	SS	SI
6	PC	SS	SI	PP
7	SI	PP	PC	SS

Table 2.3: Experimental design for testing of excitation wavelength and acetic acid volume. Excitation wavelength and acetic acid volume were tested for effects on biofilm accumulation in the following manner: coupons from runs 1-5 were examined at 492 nm using 20 mL of acetic acid (AA) (n=5) , coupons from runs 4-5 were examined at 570 nm using 20 mL of AA (n=2), coupons from runs 6-7 were examined at 492 nm and 570 nm using 6 mL of AA (n=2).

	Tests			
Run	492 nm, 20 mL AA	570 nm, 20 mL AA	492 nm, 6 mL AA	570 nm, 6 mL AA
1				
2				
3				
4				
5				
6				
7				

Optical imaging

Biofilms were imaged using a reflective light optical stereomicroscope (Model K400P, Motic, Inc.) and iSolution Lite software at 12X magnification.

Calculation of inoculum broth density

Inoculum broth density was determined according to methods from Buckingham-Meyer, et.al 2007 [23]. Inoculation broth was diluted in a serial, ten-fold dilution series. Each dilution was plated using the drop plate method where ten drops (10 μl) for each dilution were plated on a TSA plate and incubated at 37°C for 24 hrs. Countable drops were counted and a mean colony forming unit (CFU) per drop was determined. The inoculation broth density was calculated from Equation 1.

$$\text{Log}_{10}\ \text{CFU/mL} = \text{Log}_{10}\ [(\text{mean CFU/drop})/0.01\text{ml}) \times (\text{dilution factor})] \qquad (1)$$

Modification of colorimetric assay method

A colorimetric assay originally developed for quantifying biofilm accumulation on tissue culture plates was modified to quantify biofilm accumulation on the material coupons. Biofilms were grown under both static and dynamic conditions according to the methods described above. Coupons were carefully removed from incubation and rinsed in filter-sterilized water to wash any planktonic bacteria. Biofilms were heat fixed at 60°C for 1 hr. Fixed biofilms were stained with CV (Harleco's Gram Stain kit, EMD Millipore) for 10 minutes. Excess stain was removed by washing in filter-sterilized water until wash

solution was clear. Coupons were sonicated (Brunson 5510, Branson Ultrasonics Corporation, Danbury, CT) in 20 mL (n=5) and 6 mL (n=2) of acetic acid for 20 minutes to elute the stain from the adhered biofilm. A sample volume (200 µl) of the eluted stain solution from each coupon was transferred using a multichannel micropipette to a single row of wells (n=8) of a sterile, polystyrene 96-well tissue culture plate and read in a spectrophotometric microplate reader (Epoch™, BioTek® Instruments, Inc., Winooksi, VT) at a wavelength of 492 nm (n=7) and at wavelength of 570 nm (n=4). The eluted CV from each coupon was quantified by absorbance.

Statistical analysis

Effects on the data were analyzed with a generalized linear model and a binomial distribution using statistical analysis software, JMP (JMP 11.0, SAS Institute, Inc., Cary, NC) Inoculum concentration, channel position, material, flow conditions, excitation wavelength, and acetic acid volume were the factors tested for significant effects on the variable absorbance (**Appendix A**).

Crystal violet calibration curve

In order to determine the range of sensitivity of the spectrophotometric microplate reader a CV calibration study was conducted. A 100% CV solution was diluted in acetic acid in a series of ten-fold dilution steps, 10%, 1%, and 0.1% to produce a calibration curve for crystal violet. 200 µl of each concentration was loaded in a 96-well plate and

absorbance was measured in a spectrophotometric microplate reader (Epoch™, BioTek® Instruments, Inc., Winooksi, VT) at excitation wavelengths of 492 nm and 570 nm.

S. epidermidis biofilm growth curve

In order to determine a growth curve for *S. epidermidis* under the previously described experimental growth conditions a time study was conducted. Biofilms were grown under static conditions in sterile petri dishes each containing 15 mL of 30 g/L TSB. Six glass coupons were inoculated with 1 mL of *S. epidermidis* inoculum at 9.46 Log_{10} CFU/mL (high inoculation broth density). Biofilms were grown at 37°C and coupons were removed from incubation sequentially every four hours for 24 hrs. Twelve coupons were inoculated with 1 mL of *S. epidermidis* inoculum at 5.46 Log_{10} CFU/mL (low inoculation broth density). Biofilms were grown at 37°C and coupons were removed from incubation sequentially every four hours for 48 hrs. Upon removal from incubation, biofilms were fixed at 60°C for 1 hr and biofilm accumulation was measured using the colorimetric assay by eluting with 6 mL of acetic acid and measuring absorbance at 492 nm and 570 nm excitation wavelengths.

Standard curve for absorbance and bacteria concentration

In order to quantify absorbance in terms of bacteria concentration, a standard curve was necessary to demonstrate the relationship between these two variables. *S. epidermidis* inoculum at 9.96 Log_{10} CFU/mL was serially diluted in 30 g/L TSB in a 1:10 dilution series to achieve 10 dilutions of inoculum. Eleven glass coupons were inoculated with 1 mL of each inoculum concentration, including the original stock inoculum (n=11).

Biofilms were grown under static conditions in sterile petri dishes each containing 15 mL of 30 g/L TSB at 37°C for 24 and 48 hrs. Upon removal from incubation, biofilms were fixed at 60°C for 1 hr and biofilm accumulation was measured using the colorimetric assay by eluting with with 6 mL of acetic acid and measuring absorbance at a 492 nm excitation wavelength.

2.3 RESULTS AND DISCUSSION

Verification of biofilm growth under static and dynamic conditions

This study addresses the first aim (**Figure 1.1**), which was to grow biofilms under static and dynamic flow conditions. Two different metrics were applied to verify biofilm growth: imaging and consistency in inoculum broth density. Optical stereomicroscope images were taken of *S. epidermidis* biofilms grown under static and dynamic conditions on each of the four materials, as well as glass (**Figure 2.2**). These images qualitatively demonstrated biofilm growth on all four materials. Inoculation broth density was compared for all seven weeks of data collection to ensure consistency. **Figure 2.3** demonstrates the inoculation broth density for each experimental run. The average inoculation broth density for seven experimental runs was 8.4 ± 2.1 Log_{10} CFU/mL. Runs 3 and 7 reported significantly lower inoculum concentration, 5.3 Log_{10} CFU/mL and 5.4 Log_{10} CFU/mL, respectively. As a result, some variation exists between experimental runs; however, statistical analysis confirmed inoculum concentration did not have an effect on biofilm growth and subsequent absorbance in the colorimetric assay ($p>0.05$). For this reason, data from all experimental runs, despite low inoculum

concentration, were considered in the colorimetric assay analysis. It was important to note that both instances of low inoculum broth density were a result of incubator malfunction and not of user error or experimental set-up. Moreover, variations within a given material type were not dependent upon channel position within the drip flow reactor. Statistical analysis confirmed channel position did not have an effect on biofilm growth and subsequent absorbance in the colorimetric assay ($p>0.05$). Overall, these data confirm and verify the methodology for biofilm growth under both static and dynamic conditions.

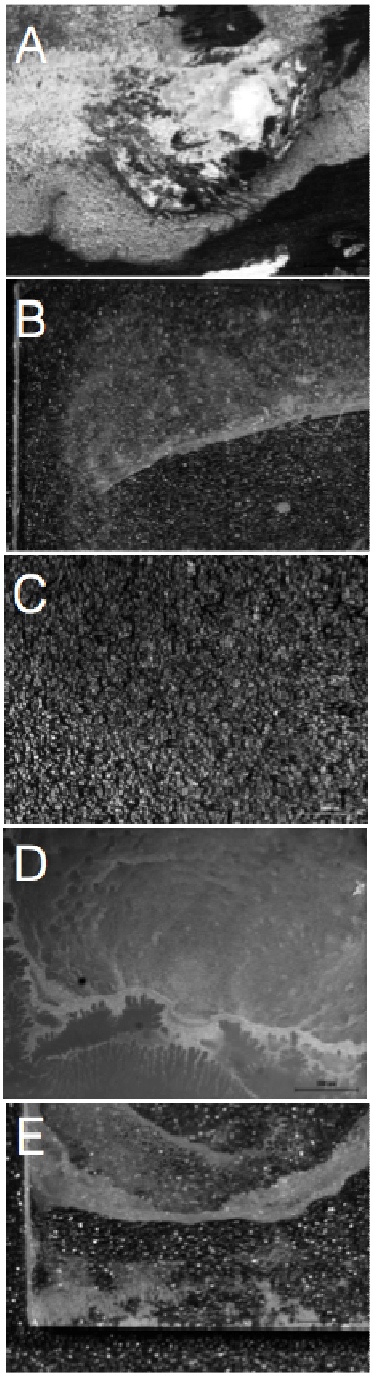

Figure 2.2: Optical stereomicroscope images of biofilm. *S. epidermidis* biofilms grown under dynamic conditions on (A) 316L Stainless Steel, (B) Polycarbonate, (C) Polypropylene, (D) Silicone, and (E) Glass at 120X magnification (scale bar is 1000 μm for each image).

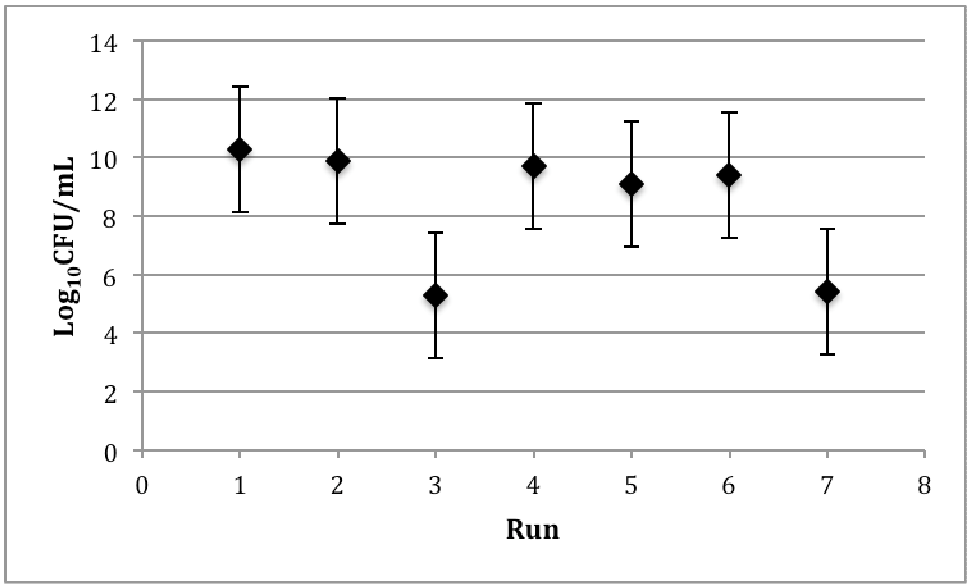

Figure 2.3: Inoculum broth density. Inoculum concentration (Log_{10}CFU/mL) was calculated for each experimental run using Equation 1. The overall average inoculum concentration for all experiments was 8.44±2.1 Log_{10} CFU/mL. This was more accurately represented as high and low inoculum concentration groups, where the average high inoculum concentration (runs 1, 2, 4, 5, and 6) was 9.68± 0.4 Log_{10} CFU/mL and the average low inoculum concentration was 5.35 Log_{10} CFU/mL (runs 3 and 7).

Modified colorimetric assay: 20 mL acetic acid, 492 nm excitation wavelength

Aims II and III in this thesis sought to modify a colorimetric assay for quantifying biofilm accumulation on various materials exposed to both static and dynamic flow conditions (**Figure 1.1**). The colorimetric assay was originally developed by Christensen, et al. (1985) to quantify adherence of clinical staphylococci isolates in a tissue culture plate (96-well plate). Bacteria were fixed and stained with CV and the absorbance of stained adherent bacteria was measured using a spectrophotometric microplate reader at 570 nm [21]. In order to accommodate the material coupons tailored specifically for the drip flow reactor, the colorimetric assay required modifications. In the modified method, use of coupons fabricated from non-opaque materials made it was necessary to first elute the CV stain from adherent biofilm grown on the material coupons and then transfer the CV stain solution to a 96-well plate, where the absorbance of the eluted solutions of CV could be measured using a spectrophotometric microplate reader. Since Christensen's method only considered biofilm grown on the bottom of the well subsequent methods have been developed to assess biofilm grown on both the bottom and the walls of the well. In this regard, acetic acid has been frequently used in the literature as a solvent to elute CV [24]. For the modified colorimetric assay, an appropriate volume needed to be determined that would release all bound CV from each biofilm, but not dilute it too much. Previous methods that used acetic acid in a 96-well plate applied a 150-200 μl volume [24]. This volume was compared to the surface area of a standard well and proportionally applied to the surface area of the selected coupons. The modified volume of acetic acid determined was 20 mL.

An initial qualitative assessment of the modified method illustrated the eluted CV solutions were well matched to the amount of adhered biofilm present on each coupon (**Appendix B.3**). **Table 2.4** shows the quantitative absorbance data from the modified method. It was important to note the absorbance value for polypropylene under dynamic conditions appeared to be outlier and a modified Thompson tau test confirmed this. The outlier was removed from all further data analysis. **Figure 2.4** illustrates absorbance values measured at 492 nm for each of the materials under both growth conditions (n=5), excluding the outlier. From these data, biofilm accumulation between materials was not significantly different ($p>0.05$). The statistical analysis confirmed that neither material selection nor flow conditions had effects on absorbance ($p>0.05$) at the 492 nm excitation wavelength.

Table 2.4: Absorbance of eluted CV solutions in 20 mL of acetic acid at an excitation wavelength of 492 nm (n=5). Five replicates of each material type with biofilm grown under both static and dynamic conditions were examined. Biofilm accumulation was detected using the modified colorimetric assay with 20 mL of acetic acid and an excitation wavelength of 492 nm. Differences in biofilm accumulation on the four materials were not significant under either dynamic ($p>0.05$) or static ($p>0.05$) conditions. For a given materials type, differences in biofilm accumulation were not significant ($p>0.05$).

		Dynamic		Static	
	Run	Absorbance, 492nm	Average Absorbance [nm]	Absorbance, 492nm	Average Absorbance [nm]
316L Stainless Steel	1	0.069	0.16±0.06	0.547	0.34±0.20
	2	0.173		0.351	
	3	0.215		0.145	
	4	0.135		0.519	
	5	0.204		0.136	
Polycarbonate	1	0.091	0.10±0.06	0.114	0.20±0.19
	2	0.145		0.134	
	3	0.179		0.095	
	4	0.055		0.551	
	5	0.048		0.129	
Polypropylene	1	1.305	0.42±0.49	0.157	0.22±0.13
	2	0.151		0.344	
	3	0.211		0.064	
	4	0.263		0.375	
	5	0.185		0.175	
Silicone Rubber	1	0.197	0.24±0.15	0.453	0.17±0.16
	2	0.316		0.167	
	3	0.459		0.064	
	4	0.191		0.107	
	5	0.05		0.075	

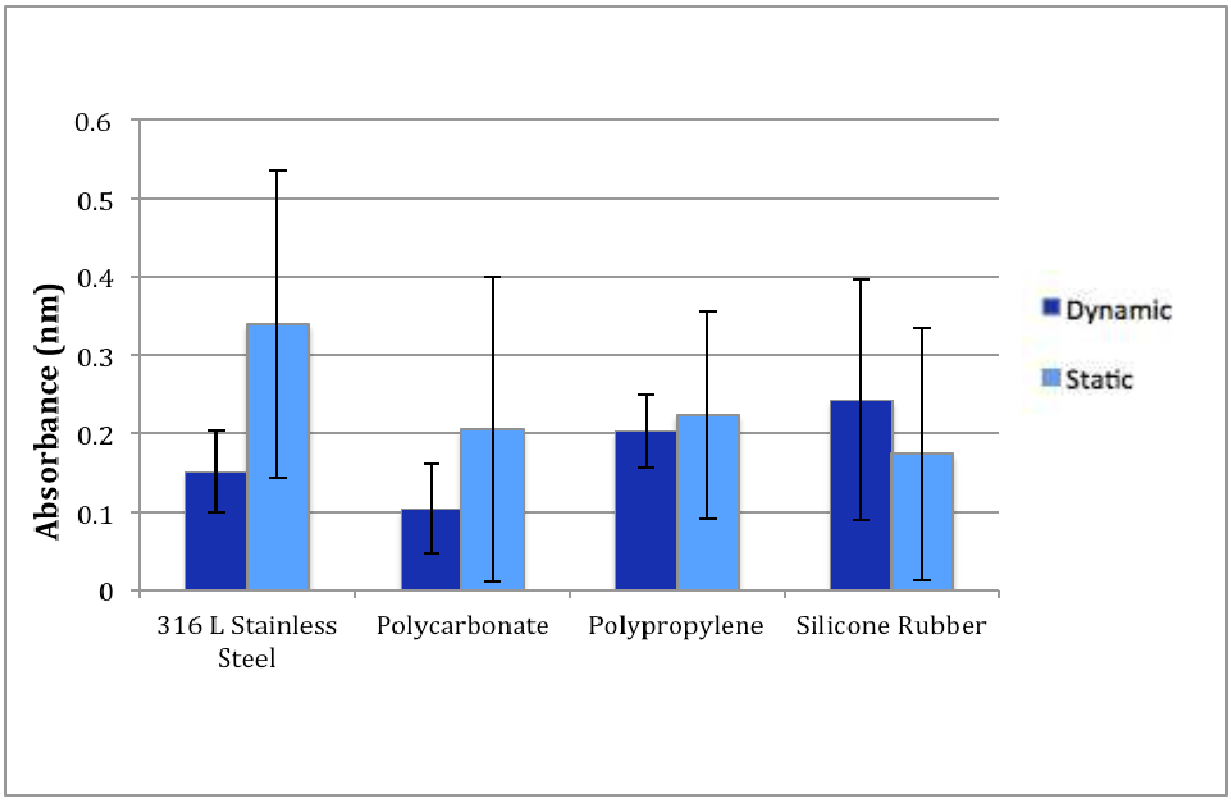

Figure 2.4: Absorbance of eluted CV solutions in 20 mL of acetic acid at an excitation wavelength of 492 nm (n=5). Graphical data excludes the outlying absorbance value, 1.305, for polypropylene under dynamic conditions in Run 1. This value was confirmed an outlier from the modified Thompsons tau test. These data demonstrate variation in biofilm accumulation for each material under both static and dynamic conditions. Differences in biofilm accumulation on the four materials were not significant under either dynamic ($p>0.05$) or static ($p>0.05$) conditions. For a given materials type, differences in biofilm accumulation under static and dynamic conditions were not significant ($p>0.05$).

The statistical analysis concluded these parameters did not impact biofilm behavior drastically enough to result in differences in biofilm accumulation. However, these two parameters are well characterized in their influence on biofilm behavior. Material characteristics, specifically surface roughness and surface energy, are well understood in their effect on biofilm adherence [15]. Generally, rougher more hydrophobic materials will develop biofilms that are more strongly adhered [15] while the opposite is true for smoother hydrophilic materials [15]. Fluid flow conditions are also well understood in their effect on biofilm adhesion. Pereia, et.al (2002) conducted a fluid flow analysis for *Pseudonomas fluorescens* biofilms under both turbulent flow (Re=5500, fluid velocity 0.5 m s^{-1}) and laminar flow (Re=2000, fluid velocity 0.2 m s^{-1}) conditions and observed distinct differences in biofilm architecture [25]. Biofilms grown under laminar fluid flow conditions will be thicker as nutrient acquisition is facilitated in these conditions, yet less dense due to sloughing. Biofilms will eventually reach a saturation point in thickness and will slough off in order to maintain viability. For this reason, biofilms in laminar flow conditions will be less resistant to detachment [25]. Biofilms grown under turbulent fluid flow conditions respond to the hydrodynamic stresses through increased production of EPS, which increases adhesion of the biofilm to its substrata [25]. Recognizing that both material selection and fluid flow conditions are known to have an effect on biofilm accumulation, these data from the current study were further analyzed.

Modified colorimetric assay: 20 mL acetic acid, 570 nm excitation wavelength

It was observed that absorbance values were very low in comparison to data reported in the literature [21]. It was, therefore, hypothesized that the CV concentration was not in the most sensitive range of absorbance for the 492 nm excitation wavelength. Using the CV calibration curve, the sensitivity of the spectrophotometer microplate reader at both 492 nm and 570 nm excitation wavelengths was determined for various CV concentrations. **Figure 2.5** shows at 492 nm there is a higher degree of sensitivity for high CV concentrations (>1%), while at 570 nm there is a higher degree of sensitivity for low CV concentrations (<1%). Recognizing that low levels of biofilm accumulation may be better detected at the 570 nm excitation wavelength, the 570 nm excitation wavelength was incorporated in the colorimetric analysis along with 492 nm. **Table 2.5** shows absorbance data for experimental runs 4 and 5 excited at 570 nm. From these data, differences in biofilm accumulation remained insignificant. Statistical analysis concluded excitation wavelength also did not have an effect on absorbance ($p>0.05$).

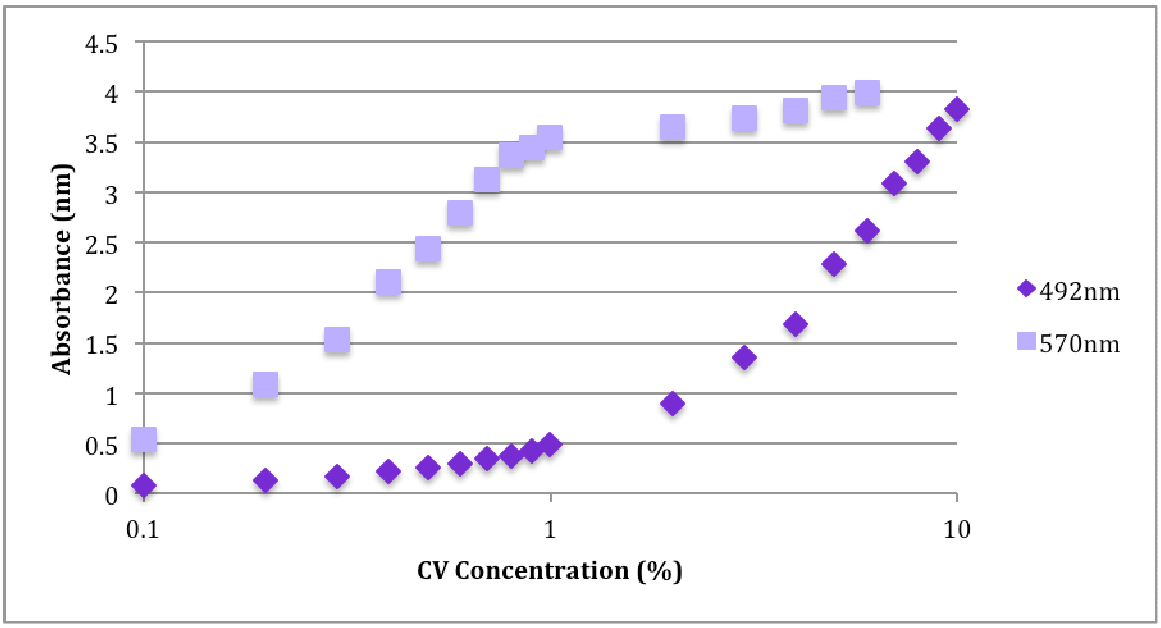

Figure 2.5: Crystal violet calibration curve. CV was diluted in acetic acid to achieve a series of ten-fold dilution steps, 10%, 1% and 0.1% to produce a calibration curve for CV concentration at excitation wavelengths of 492 nm and 570 nm. At 492 nm, the most sensitive range of detection is between 1% and 10% CV concentration. Whereas, at 570 nm the most sensitive range of detection is between 0.1% and 0.8%.

Table 2.5: Absorbance of eluted CV solutions in 20 mL of acetic acid at an excitation wavelength of 570 nm (n=2). Two replicates of each material type with biofilm grown under both static and dynamic conditions were examined. Biofilm accumulation was detected using the modified colorimetric assay with 20 mL of acetic acid and an excitation wavelength of 570 nm. Differences in biofilm accumulation on the four materials were not significant under either dynamic ($p>0.05$) or static ($p>0.05$) conditions. For a given material type, differences in biofilm accumulation under static and dynamic conditions were not significant ($p>0.05$).

		Dynamic	Static
	Run	Absorbance, 570nm	Absorbance, 570nm
316L Stainless Steel	4	0.717	3.45
	5	1.47	0.998
Polycarbonate	4	0.137	3.52
	5	0.124	0.823
Polypropylene	4	1.67	2.63
	5	1.72	1.51
Silicone Rubber	4	1.09	0.538
	5	0.123	0.375

Modified colorimetric assay: 6 mL acetic acid, 492nm and 570nm excitation wavelengths

A third approach was implemented in an effort to improve the modified colorimetric assay for detecting difference in biofilm accumulation grown under static and dynamic conditions on the selected materials. It was hypothesized that too much acetic acid would dilute the CV solution and obscure the data, thereby, making it difficult to discern differences in biofilm accumulation. This approach, therefore, proposed a decrease in the volume of acetic acid used to elute CV from adhered biofilm. **Table 2.4** reports the highest absorbance value to be 1.305. This absorbance value corresponded to a CV concentration of 3%, according to the CV calibration curve (**Figure 2.5**). A 3% CV concentration in 20 mL of acetic acid indicated 0.6 mL of CV was taken up by the biofilm. In order to optimize the detection of CV, it was necessary to have a target CV concentration within the range of high sensitivity. For a 492 nm excitation wavelength, this was a 10% CV concentration (**Figure 2.5**). Therefore, assuming the volume of CV uptake by the biofilm was constant, 0.6 mL, only a 6 mL volume of acetic volume would be needed. **Table 2.6** provides absorbance data for experimental runs 6 and 7, which used 6 mL of acetic acid, at excitation wavelengths 492 nm and 570 nm, respectively. In these data, statistical analysis reported that excitation wavelength did have an effect on absorbance ($p<0.05$). Detection of biofilm was improved when the volume of acetic acid was decreased, resulting in increased concentrations of CV. The increase in CV concentrations shifted the range of detection in the regions on the CV calibration curve where absorbance was most sensitive. **Figure 2.6** confirmed the excitation wavelengths had distinct regions of high sensitivity. Consequently, it was likely for wavelength to

have an effect when CV concentrations fell within those distinct regions. Despite the increase in sensitivity, differences in biofilm accumulation between materials were not significant ($p>0.05$). Statistical analysis of these data confirmed material selection and flow conditions remained not significant in their effect on absorbance ($p>0.05$). However, due to the low sample size for each material the power for detecting significant differences is also low ($\beta<0.8$). Consequently, if there were significant differences in biofilm accumulation it is likely they would not be detected.

Table 2.6: Absorbance of eluted CV solutions in 6 mL of acetic acid at excitation wavelengths of 492 nm (n=2) and 570 nm (n=2). Two replicates of each material type with biofilm grown under both static and dynamic conditions were examined. Biofilm accumulation was detected using the modified colorimetric assay with 6 mL of acetic acid and excitation wavelengths of 492 nm and 570 nm. Differences in biofilm accumulation on the four materials were not significant under either dynamic ($p>0.05$) or static ($p>0.05$) conditions. For a given materials type, differences in biofilm accumulation under static and dynamic conditions were not significant ($p>0.05$).

		Dynamic	Static	Dynamic	Static
	Run	Absorbance, 492nm	Absorbance, 492nm	Absorbance, 570nm	Absorbance, 570nm
316L Stainless Steel	6	0.583	0.445	3.650	3.466
	7	0.307	2.375	2.721	3.987
Polycarbonate	6	0.187	0.234	1.306	2.225
	7	0.094	0.849	0.484	3.646
Polypropylene	6	0.275	0.374	1.962	3.355
	7	0.120	1.134	0.895	3.702
Silicone Rubber	6	0.156	0.111	0.878	0.800
	7	0.065	0.107	0.275	0.725

Biofilm growth curve

In summary, modifications to both excitation wavelength and acetic acid volume in the colorimetric assay did not result in significant differences in biofilm accumulation between each material. However, a 6 mL volume of acetic acid and a 570 nm excitation wavelength provided a highly sensitive method for detecting biofilm accumulation. Recognizing the modifications of the colorimetric assay were suitable for detecting low concentrations of biofilm and did not require further modification, biofilm growth methods were investigated.

A plausible explanation for the lack of significant differences in biofilm accumulation, unrelated to the modifications of the colorimetric assay method, was biofilm growth saturation. Biofilms are well understood in their growth patterns. Generally, biofilms exhibit four phases of growth: 1) lag, 2) exponential, 3) stationary, and 4) death [26]. The lag phase occurs immediately after inoculation and persists until the bacterial population is acclimated to the environment. At this point, cell growth proceeds at an exponential rate, hence the exponential phase. The growing bacterial population doubles at regular intervals until nutrients become limiting or toxic products begin to accumulate, which is when the bacterial population enters the stationary phase. During the stationary phase, there is no net cell growth. Finally, the cells begin to lose viability and enter the death phase [26]. Therefore, if biofilm growth during the current study had reached the stationary phase and was not changing, differences in biofilm accumulation on the various materials would be difficult to discern. It was, therefore,

hypothesized that the biofilm growth period of 54 hrs was too long and resulting biofilms were in the stationary phase of growth.

Based on the results from the *S. epidermidis* biofilm growth curve generated using high and low inoculation broth densities, the time duration to initiate the stationary growth phase was determined. **Figure 2.6** confirmed that biofilms inoculated with the high inoculation broth density were saturated after 8 hrs of static growth and **Figure 2.7** confirmed that biofilms inoculated with the low inoculation broth density were saturated after 16 hrs of static growth. These growth times are considerably lower than the 54 hrs used to generate the data in the current study. The 54 hr incubation time specified by Buckingham-Meyer, et al. (2007) was necessary for growing a robust biofilm needed for determining efficacy of disinfection solutions. This thesis, however, aimed to develop a method for detecting biofilm accumulation post cleaning processes. In this regard, the duration of biofilm growth should be less than 16 hrs in order to detect low levels of biofilm accumulation on the materials. Further research is needed to determine the biofilm growth curve for each of the materials so that the appropriate time point for assessment of biofilm accumulation can be identified.

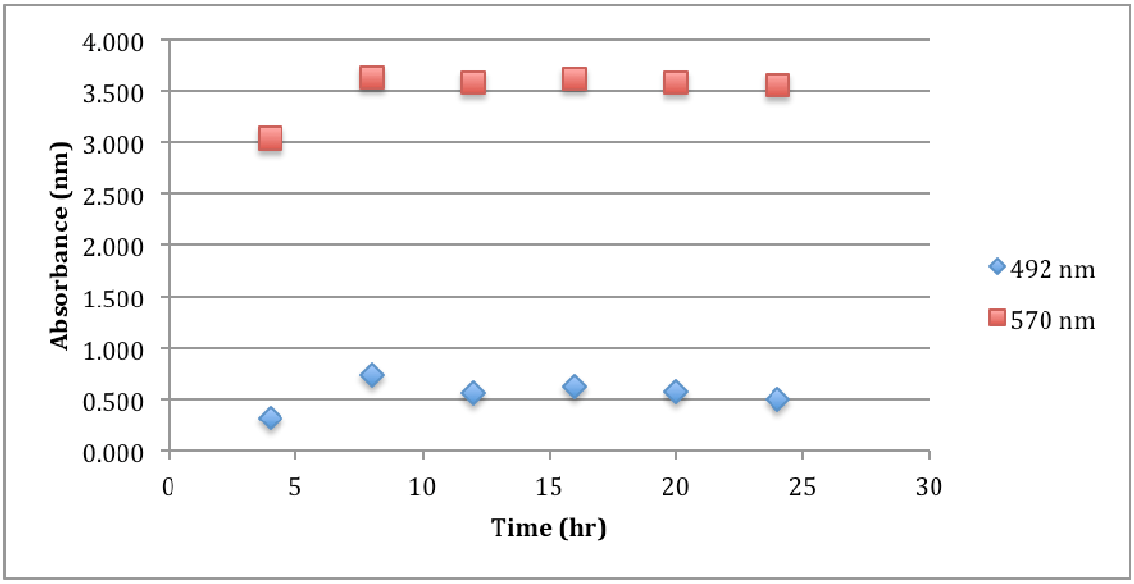

Figure 2.6: *S. epidermidis* biofilm growth over 24 hrs with a high inoculation broth density. Biofilms grown on glass coupons under static conditions. Coupons were removed from incubation every 4 hrs and biofilm accumulation was quantified using the modified colorimetric assay with 6 mL of acetic acid. At both excitation wavelengths, absorbance plateaued after 8 hrs.

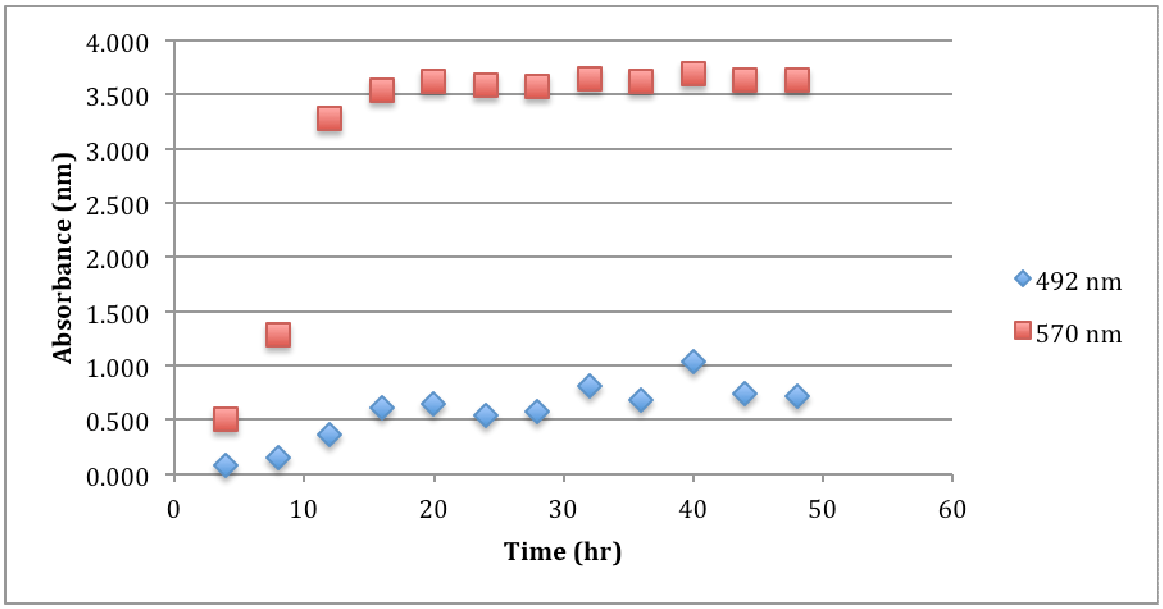

Figure 2.7: *S. epidermidis* biofilm growth over 48 hrs with a low inoculation broth density. Biofilms grown on glass coupons under static conditions. Coupons were removed from incubation every 4 hrs and biofilm accumulation was quantified using the modified colorimetric assay with 6 mL of acetic acid. At both excitation wavelengths, absorbance plateaued after 16 hrs.

Standard curve for bacteria concentration and absorbance

In order to quantify absorbance in terms of bacteria concentration, a standard curve was necessary to demonstrate the relationship between these two variables. **Figure 2.8** demonstrates the relationship between bacteria concentration and absorbance for a biofilm grown over 24 hrs and 48hrs. These data confirm a linear relationship between absorbance and bacteria concentration for concentrations in the range of of 7-9 Log_{10}CFU/mL. For all concentration less than this range, absorbance is relatively constant. This is important to note for biofilms inoculated with the low inoculum concentration (<6 Log_{10}CFU/mL) during runs 3 and 7 (**Figure 2.3**). A standard curve representing biofilms grown for shorter time periods, as discussed previously, is likely to demonstrate a linear relationship between absorbance and bacterial concentration for lower concentrations, as well. Moreover, the bacteria concentrations in **Figure 2.8** reflect the inoculum concentration and not the concentration at the end of the growth period. These data could be improved upon in future work by centrifuging and serially diluting the cells at the end of the growth period to determine the exact bacterial concentration at that point in time. Determining the relationship between absorbance and bacteria concentrations provides an accurate quantitative analysis of biofilm accumulation.

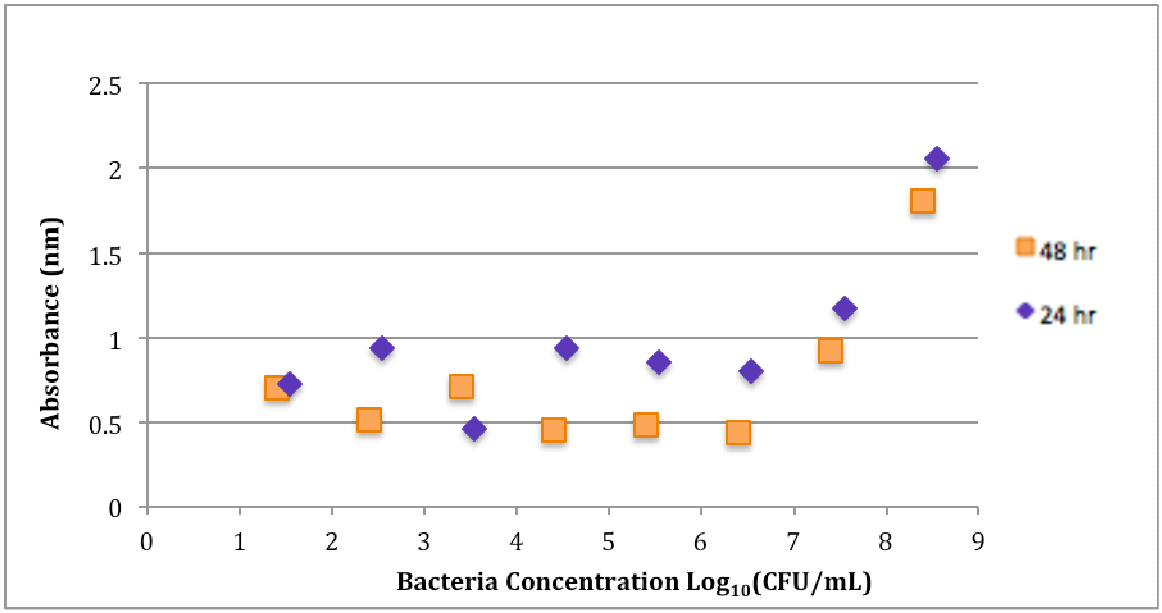

Figure 2.8: Standard curve for bacteria concentration and absorbance. Bacterial solutions were serially diluted and then cultured on glass coupons for 24 or 48 hrs. Biofilm accumulation was assessed using the modified colorimetric assay using 6 mL of acetic acid at a 492 nm excitation wavelength. A linear relationship between bacteria concentration and absorbance was observed for high concentration, 7-9 Log_{10} CFU/mL.

2.4 CONCLUSION

An established colorimetric assay for quantifying biofilms adherence to tissue culture plates was proposed as a valid method for verifying cleaning procedures required for reprocessing. However, parameters that are known to impact biofilm accumulation, material selection and fluid flow conditions, have not been previously considered in colorimetric assays for detecting biofilm. This chapter demonstrated modifications required for this assay to adequately quantify biofilm grown on large surface areas. From experimental data, it can be concluded that a 6 mL volume of acetic acid and a 570 nm excitation wavelength together provide a highly sensitive detection method for biofilms stained with CV. The high sensitivity of this colorimetric assay makes it ideal for detecting biofilm on reusable medical devices with complex design features.

Despite the high degree of sensitivity of the colorimetric assay, significant differences in biofilm accumulation between materials were not observed. The biofilm growth curve demonstrated that in order to detect significant differences in biofilm accumulation on the various materials, biofilm growth time should be reduced to 8 hrs or less. Further data is needed to determine if significant differences in biofilm accumulation on the different materials can be detected using the 8 hr incubation time.

In conclusion, the experimental work presented in this study confirmed that the modified colorimetric assay is a high sensitivity assay with potential to detect biofilm accumulation on reusable medical devices. The findings in this study also show that while material selection and flow conditions may not have an effect on biofilm accumulation, biofilm growth conditions do as well. In this regard, for future work it

would be important to assess variation in biofilm growth conditions, such as time, and how it may effect biofilm accumulation on reusable medical devices.

CHAPTER THREE

CONFOCAL IMAGING AND QUANTITATIVE ANALYSIS OF BIOFILMS ON NON-TRANSPARENT MATERIALS

3.1 INTRODUCTION

Confocal laser scanning microscopy (CLSM) is an imaging technique used for obtaining high-resolution optical images at various depths of a sample to generate 3D reconstructions. CLSM is advantageous for biofilm imaging because it can provide real-time analysis of biofilm in a natural, hydrated state. In this regard, biofilm structure can be preserved providing enhanced understanding of spatial heterogeneity, architecture, and morphology. In addition, thin optical sectioning of the biofilm can semi-quantitatively assess variations in biovolume, thickness, and viability, when appropriately labeled. Confocal imaging has been used extensively for studying variations in biofilm in differing physical and chemical environments for a variety of applications [27].

While confocal imaging has been primarily a semi-quantitative method for investigating biofilm structure, developments in image processing have refined quantitative outputs from CLSM images [27, 28, 29]. Using image-processing software, such as Image J (National Institutes of Health), pixilation intensities of biofilm with fluorescent staining can be quantified. The previous chapter discussed the development of a modified colorimetric assay and its potential application in cleaning protocols required for reprocessing reusable medical devices. Recall, the colorimetric assay utilizes a crystal violet stain that binds to bacteria cell walls of both live and dead bacteria and the amount of crystal violet bound to adhered biofilm can be quantitatively assessed through

absorbance. Comparing absorbance measurements and intensity ratios for a given biofilm could demonstrate a direct relationship between the colorimetric assay and confocal imaging effectively validating the modified colorimetric assay as a method for detecting biofilm accumulation on reusable medical devices.

However, in order to obtain accurate quantitative data, fluorescent imaging techniques for biofilms needed to be optimized. Though there are many published methods for imaging biofilm using CLSM, there are few that observe biofilm grown on non-transparent materials. Scanning electron microscopy (SEM) is a commonly used imaging modality because it can provide high-resolution images of cellular morphology on non-transparent materials. However, because SEM requires fixation it can alter structure and cellular spatial variation within the biofilm [30]. Implementation of a glass interface, whether through cover slipping or a glass-bottom petri dish, has been shown to be an effective method for CLSM imaging of biofilm on non-transparent materials [31]. The objectives of this study were to demonstrate imaging processing of fluorescent intensities as a means to quantify biofilm accumulation and to optimize biofilm imaging techniques for biofilms grown on non-transparent materials through a step-wise approach.

3.2 MATERIALS AND METHODS

Bacterial species/strains and culture preparation

Staphylococcus epidermidis ATCC 12228 stock cultures were streaked on Tryptic Soy Agar (TSA) plates and incubated overnight at 37°C to obtain isolated colonies. A single colony was transferred to 30 g/L Tryptic Soy Broth (TSB) media and grown overnight in a shaker incubator at 37°C and 125 rpm to a high inoculum concentration of approximately 9 Log_{10} CFU/mL. The overnight cultures were used to inoculate the experimental coupons. Stock cultures were frozen in 1:1 of 20% sterile glycerol and media. Bacteria were recovered in 10 mL of media and incubated for 24 h at 37°C.

Live/Dead assay verification on glass-bottom fluorodishes

A glass-bottom fluorodish (Model No. FD35-100, World Precision Instruments, Inc., Sarasota, FL) was inoculated with 1 mL of *S. epidermidis* inoculum at a high inoculum concentration of approximately 9 Log_{10} CFU/mL and incubated overnight at 37°C. Biofilm was stained with a fluorescent viability stain (FilmTracer™ LIVE/DEAD® Biofilm Viability Kit, L10316, Invitrogen) according to the manufacturer's instructions. Biofilms were excited with a white light laser at 480 nm and 535 nm excitation wavelengths using a 63X oil-immersion lens (HcPl APO CS2 NA1.4) with the Leica SP8X-MP confocal microscope (Leica Microsystems, Buffalo Grove, IL).

Cover slipping verification on rectangular glass coupons

The edges of glass coupons (25 x 75 x 1 mm) were first masked with Teflon tape to prevent biofilm growth where the coverslip would later be adhered. Coupons were placed in sterile petri dishes, each containing 15 mL of 30 g/L TSB. Coupons were inoculated with 1 mL of *S. epidermidis* inoculum at a high inoculum concentration of approximately 9 Log_{10} CFU/mL and incubated at 37°C for 48 hrs. Coupons were removed and rinsed in filter-sterilized water to remove any planktonic cells. Biofilms were stained with a fluorescent viability stain (FilmTracer™ LIVE/DEAD® Biofilm Viability Kit, L10316, Invitrogen) according to the manufacturer's instructions. The Teflon tape was removed and glass coverslips were affixed using Valup wax. Biofilms were excited with a white light laser at 480 nm and 535 nm excitation wavelengths using a 63X oil-immersion lens with the Leica TCS SPE (Leica Microsystems, Buffalo Grove, IL) and a 20X lens with the Leica SP8X-MP confocal microscope (Leica Microsystems, Buffalo Grove, IL). Various laser, stitching, and Z stack configurations were applied for determining optimal image settings for cover-slipped biofilms.

3.3 RESULTS AND DISCUSSION

Biofilms were initially grown and imaged in a glass-bottom fluorodish to provide a standard for comparison to biofilms grown on non-transparent materials and imaged using a cover slipping method. Biofilms were stained with a viability stain using syto 9 and Propidium Iodide labels. Syto 9 is a DNA binding dye that indicates live cells through green fluorescence emission, while propidium iodide is a DNA binding dye that

only penetrates permeabilized membranes and indicates dead or dying cells through red fluorescence emission. 3D reconstructions of the biofilm demonstrated a biofilm approximately 40 μm thick (**Figure 3.1-A, B**). Additionally, the maximum intensity projection image in **Figure 3.1-C** showed high pixel intensities (orange/yellow pixels) throughout the biofilm. This result indicated a well-formed and spatially diverse biofilm and provided preliminary verification of the staining and imaging techniques.

Aim II (**Figure 1.1**) of this thesis sought to develop methods for quantitatively assessing biofilm accumulation using CLSM. To achieve this aim, individual slices of the 3D reconstruction were analyzed using image processing software, ImageJ. High-resolution, RGB images from each fluorescent channel were captured and converted to 8-bit grey scale images. Background fluorescence was subtracted from each grey scale image using the Rolling Ball method at a 10-pixel radius. The Otsu Threshold method was applied to detect edges in intensity to create a binary mask for both live and dead channels. The binary mask is a black and white image where black pixels represent signal and white pixels represent no signal (**Figure 3.2**). From the binary mask, pixels were counted as regions of interest (ROI) to determine cell counts and percent area of cell coverage. Percent area was calculated based on the average size of the ROI. ROI size varied from large clumps to discrete particles as a result of staining (**Figure 3.2**). The quantitative outputs for a single slice at 9.9 μm are shown in **Table 3.1.** There were significantly more live cells than dead cells, 1,923 and 908, respectively. Considering area coverage, live bacteria covered 82% of the defined 200 μm x 200 μm area, while dead bacteria only covered 18% of the defined area. Overall, these data confirmed the

image processing methods were an accurate method to quantify cell counts within a 3D biofilm sample. These data could be obtained for the entire 3D stack through automated processing, which would provide quantitative information related to total biofilm accumulation.

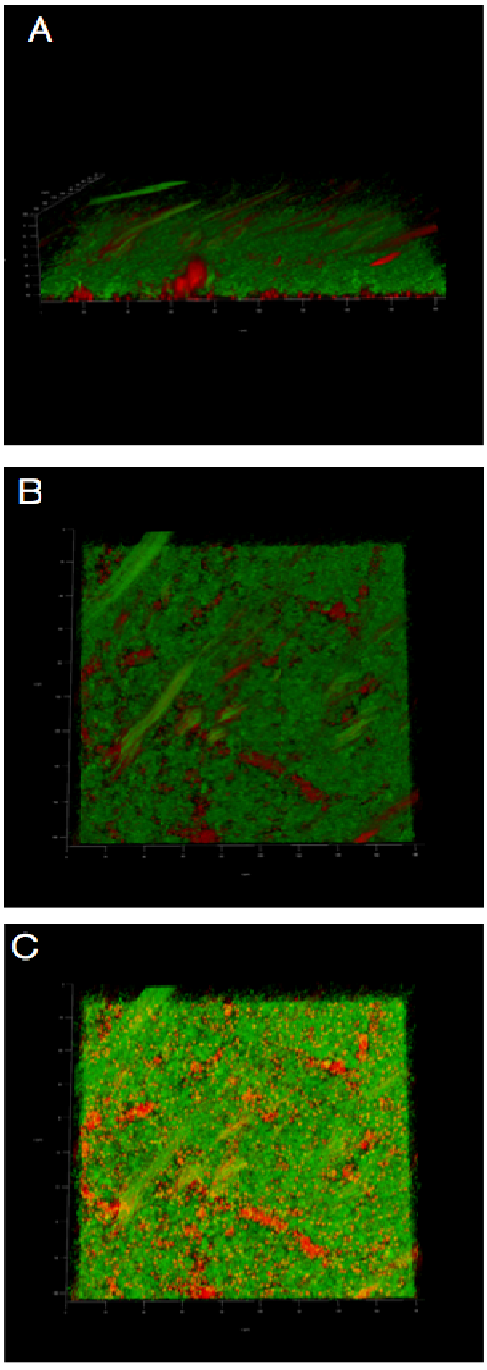

Figure 3.1: 3D CLSM images of *S. epidermidis* biofilm at 63X magnification on glass-bottom fluorodish. A) and B) 3D Z-stacks of biofilm stained with BacLight viability assay that labels live cells green and dead cells red. C) A maximum intensity projection of z-stack highlights presence of high intensity pixels in variations of orange and yellow. Image scale is 200 μm x 200 μm.

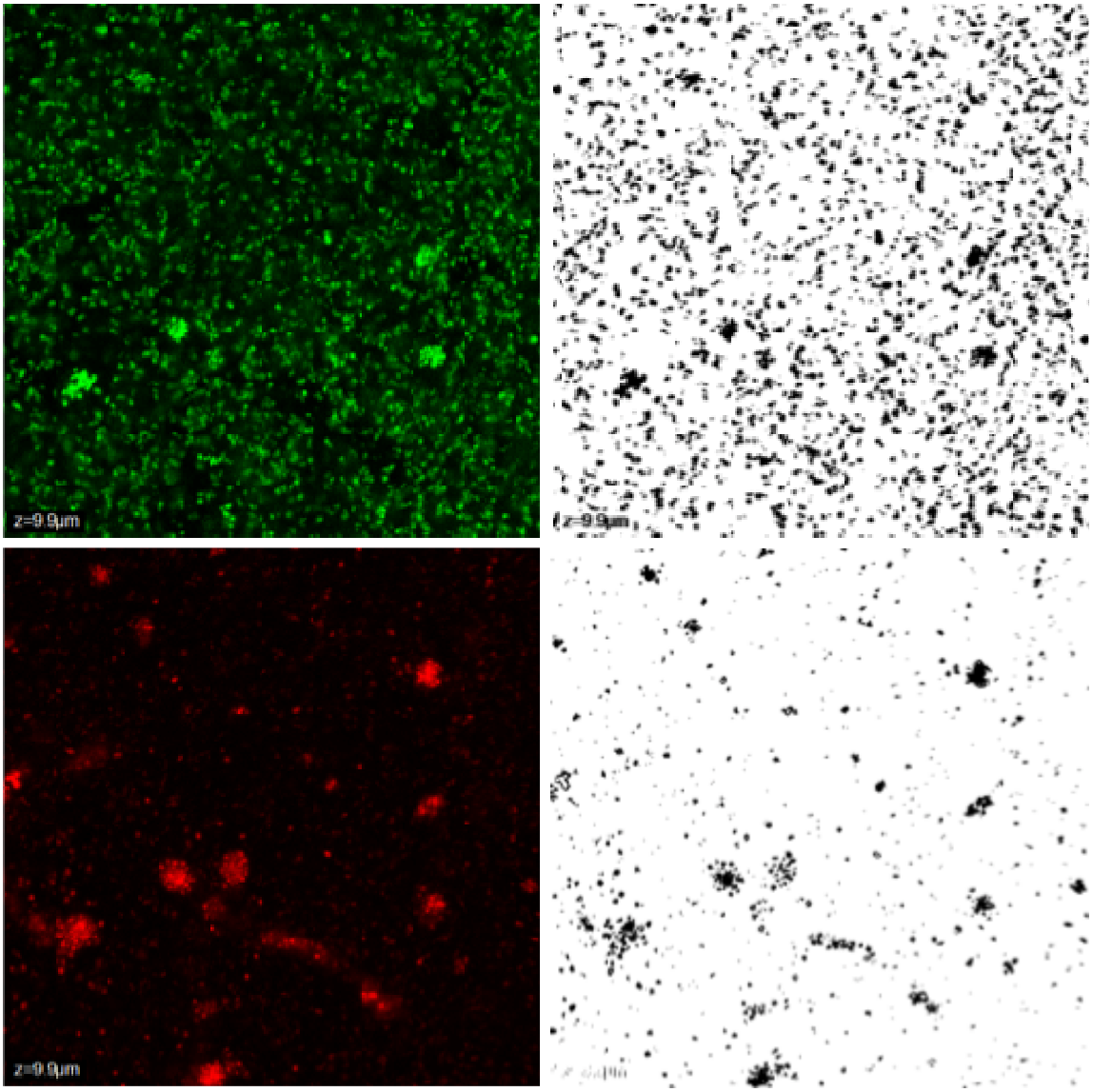

Figure 3.2: Processed CLSM images of *S.epidermidis* biofilm at 9.9 µm. CLSM images were converted to binary (black and white) images using ImageJ software. (Top) Initial and binary images of live bacteria cells stained with syto 9. (Bottom) Initial and binary images of dead bacteria cells stained with propidium iodide. Image scale is 200 µm x 200 µm.

Table 3.1: *S. epidermidis* biofilm cell quantification at 9.9 μm slice of CLSM 3D Z-stack. Image processing outputs yield a total particle count of 2,831 cells with 68% being live cells and 32% being dead cells. Considering the variation in size of the ROI, % area of cell coverage for 200 μm x 200 μm area was also determined. Live cells covered 82% of the defined area, while dead cells covered 18% of the defined area.

Slice	Count	% Cells	Average Size of ROI	Total Area	% Area
Live	1,923	68	1,327,207	2,552,218,241	82
Dead	908	32	635,744	57,725,591	18
Total Cells	2,831				

Aim III (**Figure 1.1**) of this thesis sought to apply imaging methods for biofilms on non-transparent materials. In this regard, various techniques were implemented to obtain optimal biofilm images. In order to image biofilms on non-transparent materials a cover slip is required to provide a glass interface for light transmission to the sample. To adequately adhere the cover slip to the coupon without compressing the biofilm, Teflon tape was first applied to the coupon to mask biofilm growth. Prior to imaging, the Teflon tape was removed and Valup wax was applied to affix the edges of the glass cover slip to the coupon. While the tape and wax method did improve adherence of the coverslip and, subsequently, focus, there were two distinct challenges associated with this method. First, placement of the coverslip in a perfect, level orientation was difficult. As a result, there was a "tilt effect" which caused variation in detected intensity throughout the sample. Laser settings should be optimized for a given biofilm based on the staining method and substrate material. However, when scanning in the z-plane those specified settings were not captured when there were changes in the z distance between the coverslip and the biofilm. This variation resulted in loss of signal and, subsequently, gaps in the detected intensity. **Figure 3.3** demonstrates the gaps in detected intensity signal in both the green and red fluorescent panels where there was no detection in the 0-60 μm region in the x-direction and then apparent detection in the 60-200 μm region in the x-direction. For imaging processing this would yield significant error in the quantitative data outputs.

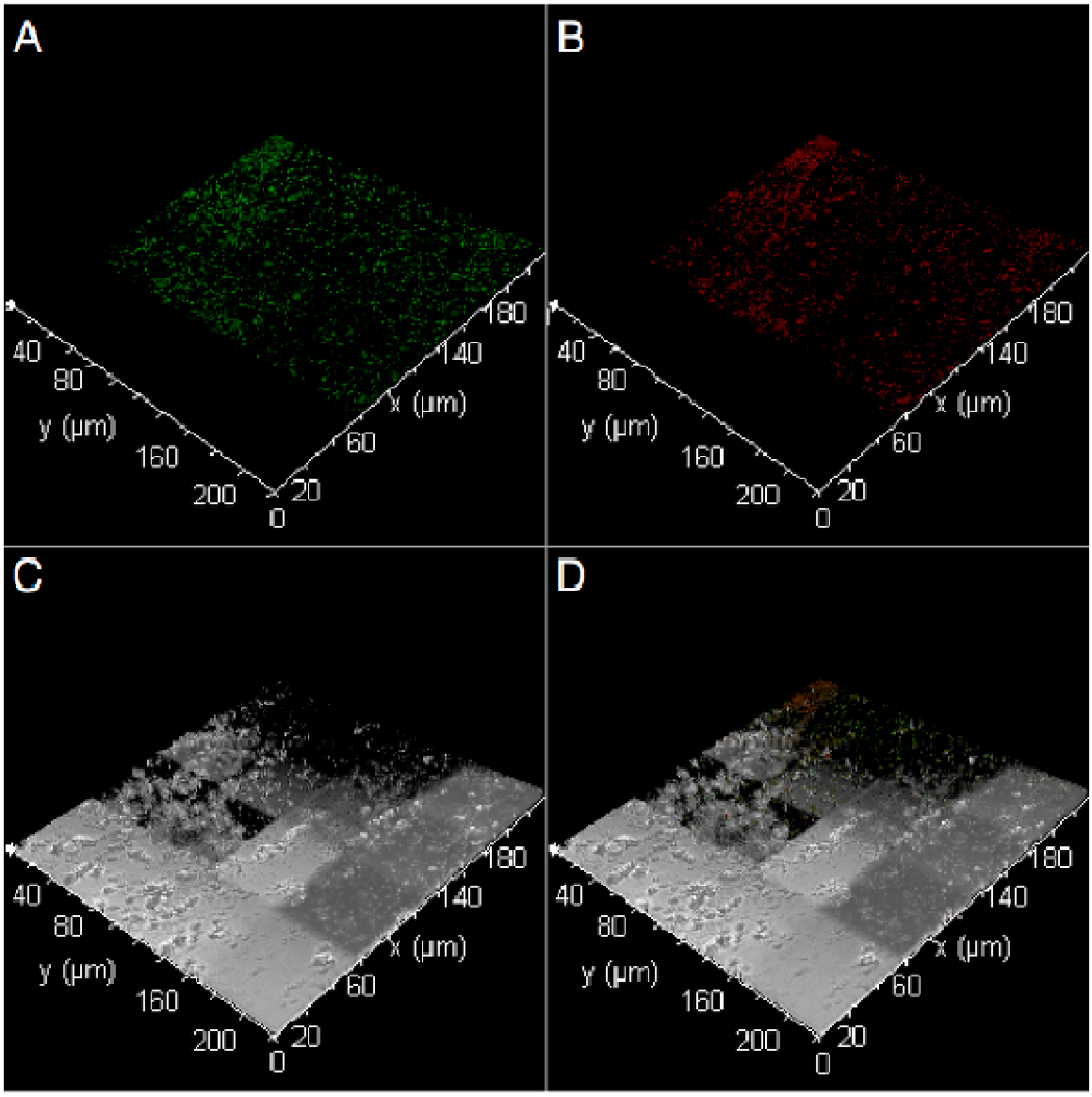

Figure 3.3: 4 x 4 tile scans of *S. epidermidis* biofilm on rectangular glass coupon at 63X magnification. A) Syto 9 fluorescent label (live cells) B) Propidium Iodide fluorescent label (dead cells). C) Differential interference contrast image D) Overlay of images A-C. Image scale is 200 µm x 200 µm.

The images shown in **Figure 3.3** were taken as an automated stich of a 4 x 4 tiled region within the biofilm sample. It was thought that reducing the area of the tiled region would mitigate the "tilt" effect. **Figure 3.4** shows a 3 x 3-stitched region where improved detection was observed. However, this image introduced another observed artifact: "the puzzle piece effect." Stitching is a way to automate image capture so that a statistically significant region of the biofilm can be analyzed. This method ensures imaging of regions in the middle, as well as regions on the edges of the biofilm. However, because the biofilm sample was sparse and non-uniform the software did not have an accurate frame of reference to stich the correct pixels. **Figure 3.4** shows severe discontinuity in the third tiled region. Discontinuity in the stitch would make it difficult to accurately quantitatively assess the biofilm. To address these two challenges biofilm samples were imaged at a lower magnification, 20X. A lower magnification would result in less distinct morphology, however, it would allow capture of a large region without having to modify laser settings, thereby, potentially reducing the effect of the cover slip tilt and the discontinuity in stitching. Despite this, biofilm imaged at 20X showed significant artifacts in the intensity in both the green and red fluorescent panels, as shown in **Figure 3.5.** Intensity variation could be observed even within a single tiled region of biofilm. Overall, these methods resulted in poor quality images with intensity artifacts that would yield inaccurate quantitative assessment of a biofilm sample.

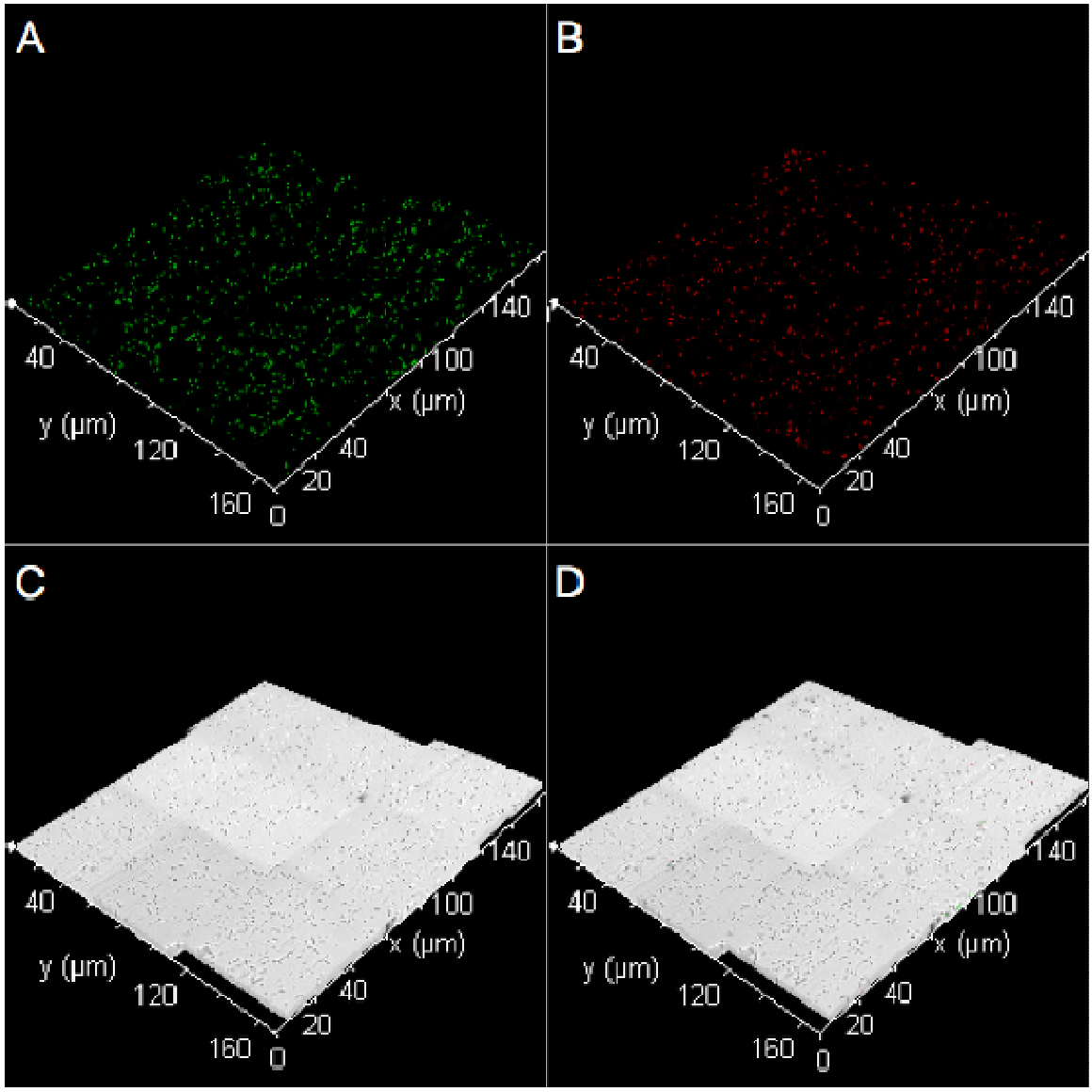

Figure 3.4: 3 x 3 tile scans of *S.epidermidis* biofilm on rectangular glass coupon at 63X magnification. A) Syto 9 fluorescent label (live cells) B) Propidium Iodide fluorescent label (dead cells). C) Differential interference contrast image D) Overlay of images A-C. Image scale is 200 µm x 200 µm.

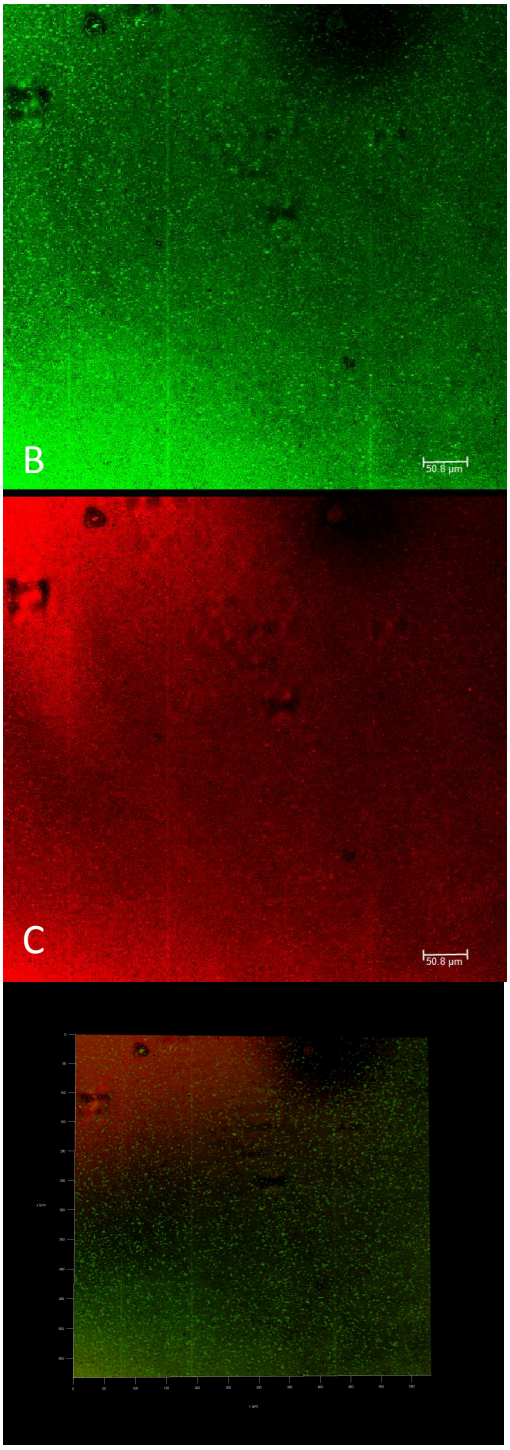

Figure 3.5: 5x5 tile scans of *S.epidermidis* biofilm on rectangular glass coupon at 20X magnification, A) Syto 9 fluorescent label (live cells) B) Propidium Iodide fluorescent label (dead cells). Scale bar is approximately 50 µm. C) Overlay. Each section is approximately 600 µm x 600 µm.

3.4 CONCLUSION

A step-wise approach for optimizing imaging techniques was used to image biofilms on non-transparent materials, quantify the amount of bacteria cells present throughout a full-thickness biofilm, and localize the live/dead cells relative to the coupon substrate. Using publically-available imaging software (ImageJ) and common image processing techniques for thresholding and masking, it was possible to determine percent area of cell coverage within the biofilm distributed over the substrate surface area. Overall, the image processing methods were suitable for quantifying cell counts within a 3D biofilm sample and could be used to gain quantitative information related to total biofilm accumulation.

While an optimal method for imaging biofilm on rectangular glass coupons was not defined, this approach generated a clearer understanding of the realities of biofilm imaging using CLSM. Glass-bottom dishes provided a usable interface for imaging biofilm on non-transparent materials without disrupting the film, whereas, cover slipping was cumbersome and resulted in many image artifacts. A proposed solution for optimizing biofilm imaging techniques on the material coupons described in this thesis is to redesign the rectangular coupons machined for the drip flow reactor to a more suitable configuration for a glass-bottom fluorodish. Optimal methods for imaging biofilms on non-transparent materials are necessary for obtaining accurate quantitative data for assessment of biofilm accumulation. Proof of-concept data showed that image processing of biofilms could quantify pixilation intensities to determine biofilm accumulation. This data could be used in the future to validate the colorimetric assay for detecting biofilm

accumulation for high-throughput industry validation methods for cleaning of reusable surgical instruments.

CHAPTER FOUR

ENGINEERING AND COMMERCIAL SIGNIFICANCE

4.1 INTRODUCTION

The broad objective of this thesis was to deliver a simple, cost-efficient method suitable for detecting biofilms on complex reusable medical devices in a high-throughput industry setting for the purpose of validating cleaning methods required for reprocessing. The purpose of this chapter is to demonstrate the significance of the broad objective as it relates to improved outcomes of medical device reprocessing.

Engineers seek to design for function and performance of their product. End-user needs are identified and designs are manifested to meet those needs. For reusable medical devices, the paradigm for device design should not solely concern function and performance. Instead, design decisions need to concern reducing biofilm accumulation and improving feasibility for cleaning. As discussed in Chapter 1, reusable medical device designs should consider reprocessing from the very early stages of device development. The first objective of this chapter is to demonstrate the impact of design considerations, such as geometry and surface texture, on biofilm accumulation and the resulting implications for medical device reprocessing outcomes. The second objective of this chapter is to demonstrate the colorimetric assay as a simple, inexpensive method to improve both human factors and cost considerations for reprocessing.

4.2 DESIGN CONSIDERATIONS FOR REUSABLE MEDICAL DEVICES

Geometry and fluid flow phenomena

The behavior of fluid flow can be described as either laminar or turbulent. At low velocities fluids tend to flow without lateral mixing and there are no crosscurrents or eddies [32]. This flow regime is described as laminar. At higher flow velocities mixing does occur resulting in crosscurrents and eddies. This flow regime is described as turbulent [32]. The conditions under which fluid flow transitions from the laminar regime to the turbulent regime are defined by a unitless parameter, Reynolds number (Re):

$$\mathrm{Re} = \frac{D\bar{V}\rho}{\mu} \qquad (1)$$

where D = diameter of the tube
$\bar{V}$ = average linear velocity of the liquid
ρ = density of the liquid
μ = viscosity of the liquid

Flow is always within the laminar regime for Reynolds numbers less than 2,100 and within the turbulent regime for Reynolds numbers greater than 2,100 [32].

As discussed in Chapter 2, many reusable surgical devices will operate under flow conditions. A principle example is the flexible endoscope. Flexible endoscopes have been used in minimally invasive surgery since the 1960s [33]. However, it wasn't until 1988 that the American Society for Gastrointestinal Endoscopy in conjunction with the American College of Gastroenterology published the first guidelines for cleaning and disinfection of GI endoscopes [33]. Flexible endoscopes have unique designs, which

make them especially challenging for reprocessing. Consequently, they have been studied extensively in regard to cleaning methods.

There are a wide variety of flexible endoscopes that are specified for many different surgical applications. Some flexible endoscopes are used only for viewing and diagnostic purposes, while some are designed with conduits for laparoscopic instruments. Despite the variety in application, flexible endoscopes generally have the same basic structure and function. There are three main components: the control section, the insertion tube, and the connector section [34]. The control section is where the operator can control the primary functions of the device such as, angulation of the instrument tip, suction, water flow, and image capture. Additionally, the control section provides the entry point for auxiliary tools. The insertion tube is a flexible shaft that allows passage of the auxiliary tools, as well as suction and fluids. Finally, the connector section attaches the endoscope to the electrical, CO_2, air/water, and light sources [34]. The most critical feature of the flexible endoscope, as it relates to biofilm formation, is the suction/biopsy channel. The suction/biopsy channel is primarily used to remove blood and tissue. For this reason, it is the most likely component of the flexible endoscope for biofilm accumulation to occur. For the purpose of providing a first-level understanding of fluid dynamics through a flexible endoscope the suction/biopsy channel has been simplified into a smooth pipe model with one-dimensional flow, as shown in **Figure 4.1**.

A principle mathematical property of flow dynamics is continuity, or conservation of the mass flow rate, $\dot{M}$ The mass flow rate is a function of fluid density (ρ), velocity (v), and the cross-sectional area of the pipe (A). Where,

$$\dot{M} = \rho v A \tag{2}$$

Conservation of mass flow states the rate of mass flow in is equal to the rate of mass flow out, (3)

$$\sum_{IN} \dot{M} = \sum_{OUT} \dot{M}$$

Using **Figure 4.1** as a model for one-dimensional flow through a suction/biopsy channel of a flexible endoscope in combination with reported inner diameter specifications and a volumetric flow rate from commercialized products a representative flow regime through a flexible endoscope channel can be characterized.

To characterize the flow regime through the model channel, the flow velocity must first be determined. The fluid velocity is defined as the volumetric flow rate divided by the cross sectional area of the channel,

$$V = \frac{Q}{A} \tag{4}$$

where,

$$A = \frac{\pi}{4} d^2 \tag{5}$$

From Equations (2), (3), (4) and (5) the flow velocity can be derived. The fluid density and the diameter are constant throughout the pipe, therefore,

$$Q_{in} = v_{out} A_{out} \tag{6}$$

The fluid velocity, *v*, and the known diameter, *d*, are used to solve for Re using Equation (1).

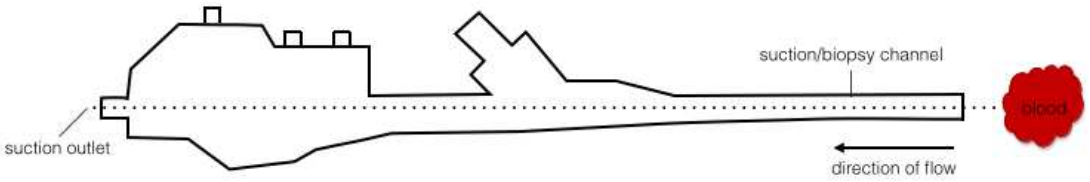

Figure 4.1: Schematic of blood flow through suction channel of flexible endoscope. In this model flow is one-dimensional, the pipe is smooth with a constant diameter, and the mass flow rate is conserved.

From a design point, it is important to consider that decreasing the channel diameter of the scope is optimal for many minimally invasive procedures. Manufacturers of flexible endoscopes often have a product line of “slim” or “ultra slim” scopes where channel diameters specifications are altered to accommodate more precise laparoscopic instrumentation. To demonstrate the effect of diameter variations on fluid flow conditions a variety of endoscope diameters were incorporated into the model and mathematical equations to yield corresponding Reynolds numbers and flow regimes.

Table 4.1 shows that for a constant volumetric flow rate, Q, as the inner diameter (ID) of the channel decreases by 3.8 mm, the Reynolds number increases by a factor of 10. The flow regime produced by these conditions is turbulent. As noted by Pereira, et.al (2002) biofilms grown under turbulent flow tend to be denser and more strongly adhered to their substrate compared to biofilms grown under laminar flow [25]. Purevdorj, et.al (2002) also observed that turbulent biofilms tend to form large streamlined patches in a confluent monolayer with some filamentous streamers [35]. It is evident that under turbulent flow there is greater accumulation of biofilm [24,35]. Devices that are designed to meet a “slim” or “ultra slim” specification will typically operate under turbulent flow and, so, must also consider the resulting effects of biofilm accumulation.

A simplified model facilitates the understanding of fluid dynamics through a straight channel. However, in reality flexible endoscopes are not rigid pipes. Their curvatures are complex, which is why they are such a challenge for reprocessing. An interesting study by Drescher, et.al (2012) illustrates how biofilm accumulation around corners can cause catastrophic disruptions of flow [36]. Using a model microfluidic flow

a system, Drescher, et.al (2012) showed that biofilm accumulation on pipe walls only marginally affects flow rate through the channel; however, biofilm streamers that form under turbulent flow around corners rapidly expand and drastically impede flow [36]. Rapidly expanding biofilm streamers in curved regions of a flexible endoscope has considerable consequences not only on the operating flow system, but also for cleaning during reprocessing.

The complexity of biofilm hydrodynamics creates many questions for researchers as they seek to understand how biofilms change in varying environments. Fully understanding variation in biofilm structure continues to elude researchers, yet for many applications it will provide the answers needed for improving industrial systems. For reusable surgical instruments, specifically, it is evident that fluid flow phenomena impacts biofilm accumulation and, therefore, must be considered in the engineering principles related to design of these devices.

Table 4.1: Variations in Reynolds number and flow regime with change in inner diameters in flexible endoscopes. Inner diameters of instrument channels and suction/biopsy channels from a variety of commercially available flexible endoscopes [34] and a volumetric flow rate from a commercially available endoscopic suction pump [37] were used to determine variations in Reynolds number and flow regime.

Constants		ID (mm)	ID (m)	V (m/s)	RE	Regime
Q [L/min]	20	4.8	4.8E-03	18.4	26677	Turbulent
Density, Blood [Kg/m3]	1056	4.2	4.2E-03	24.1	30488	Turbulent
Viscosity, Blood [Pa s]	3.5E-03	4.0	4.0E-03	26.5	32013	Turbulent
		3.8	3.8E-03	29.4	33698	Turbulent
		3.2	3.2E-03	41.4	40016	Turbulent
		3.0	3.0E-03	47.2	42684	Turbulent
		2.8	2.8E-03	54.1	45733	Turbulent
		2.2	2.2E-03	87.7	58205	Turbulent
		2.0	2.0E-03	106.1	64026	Turbulent
		1.8	1.8E-03	131.0	71140	Turbulent
		1.2	1.2E-03	294.7	106710	Turbulent
		1.0	1.0E-03	424.4	128052	Turbulent

Surface texture

Material characteristics, specifically surface roughness, are known to have an impact on biofilm accumulation. In this thesis, biofilm accumulation was quantified on four different materials with varying surface roughness (316L Stainless Steel= 0.372 μm, Polycarbonate= 0.01 μm, Polypropylene= 1.77 μm, and Silicone Rubber= 0.308 μm). It has been previously discussed that biofilm accumulation is greater for rough materials compared to smooth materials. However, Wu et al. (2011) highlights, more specifically, the effect of surface texture on biofilm accumulation [31]. Wu, et al. investigated the differential response of *S.epidermidis* and osteoblasts to varying surface modifications to titanium femoral stems. Four different surface modifications with varying surface roughness were compared: polished (R_a=0.006 μm), satin (R_a = 0.830 μm), grit blasted (R_a =11 μm), and plasma sprayed (R_a=33 μm) (**Figure 4.2**).

Using CLSM, Wu, et al. analyzed percent coverage of *S.epidermidis* on each substrate and found the satin finish had the highest percent coverage followed by grit-blasted, plasma-sprayed, and then polished. Though the plasma sprayed finished was significantly rougher compared to the satin finish, Wu, et al. (2011) demonstrated that the surface texture profiles of these two finishes varied dramatically.

The satin texture profile is macroscopically smooth, but microscopically has a lateral roughness profile with concave valleys that increase the bacteria-surface contact area [31]. In contrast, the plasma sprayed texture profile is very macroscopically rough with curvature profiles that are low and convex, which are considerably larger than the bacterial cell [31]. Essentially, Wu, et al. (2011) shows that bacterial adhesion increases

more when the surface texture profile is well matched to the bacteria morphology. In his analysis of osteoblast response, Wu, et al. (2011) found contrasting behavior in the colonization of the osteoblasts. The osteoblasts demonstrated higher percent coverage on the plasma sprayed surface finish compared to the satin finish. Overall, the surface modifications vary in roughness, but it is the differences in the macroscopic and microscopic surface profiles that impact biofilm accumulation.

Interested in biomaterials-associated infections as a leading failure mode of implants, Wu, et al. (2011) aimed to investigate the importance in roughness not only to osseointegration, but also to bacterial adhesion. Titanium surface modifications were originally incorporated into femoral stem design as a means to promote osseointgerance to preclude loosening and improve implant stability. Through his results, Wu et al. (2011) eloquently illustrated that design choices that are targeted towards improving device function and performance can have underlying implications for biofilm formation. Understanding the effect of design choices as an engineer must be well understood when designing reprocessed devices.

In surgical instrumentation, surface texture can be integrated into the design to augment device performance and improve surgeon experience. For example, texture can be incorporated into ergonomic handle designs that feature more comfortable grips during long procedures [38]. Surface textures are known to improve grip for soft tissues, which is important for biopsy forceps [38]. Additionally, more dramatic texture modifications can increase tactical sensitivity between the surgeon's hand and the instrument, which helps to reduce applied pressure to the surgical site [38]. For devices

that will be reused, it is imperative to fully understand the implications of texture and how it may impact biofilm accumulation.

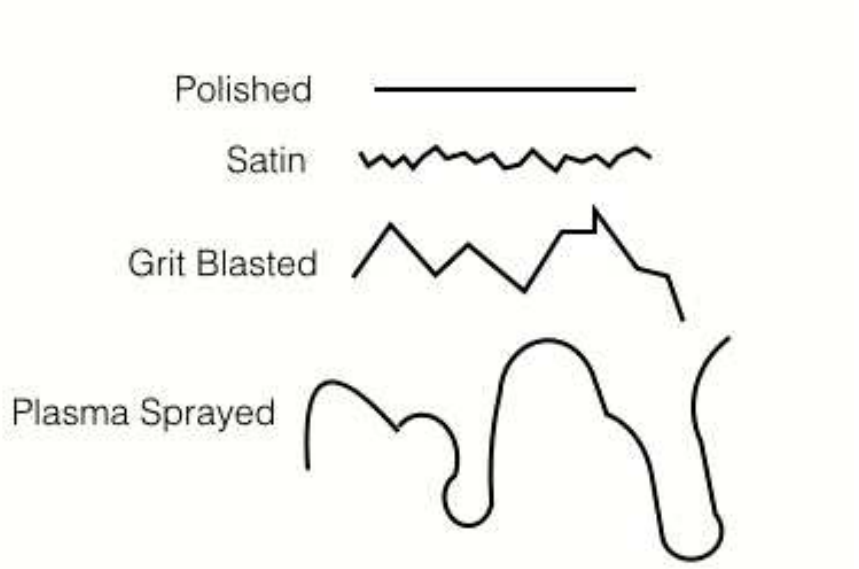

Figure 4.2: Schematic of the texture profiles of four titanium surface modifications (adapted from Wu, et al. 2011) [31]. Polished is the smoothest (R_a=0.006 μm), followed by satin (R_a = 0.830 μm), grit blasted (R_a =11 μm), and then plasma sprayed (R_a=33 μm).

4.3 HUMAN AND ECONOMIC FACTORS FOR REPROCESSING REUSABLE MEDICAL DEVICES

Human Factors

When reprocessing reusable medical devices, human factors matter. As discussed in Chapter 1, OEMs are required by the FDA to provide validated reprocessing protocols and IFU documents for every reusable device. These IFUs are intended to provide detailed instructions according to standardized methods for how to reprocess the specific device. However, lack of specificity, complicated instructions and discrepancies from standardized methods have made it extremely difficult to follow manufacturers' instructions [13]. The Central Sterile Processing Department at Johns Hopkins reprocesses at least 14,000 different reusable devices. Despite this large inventory, reprocessing technicians at that facility admit to working from memory or hearsay because of the confusing nature of the IFUs [13]. Despite that the FDA requires validation testing for human factors in reprocessing protocols, there is still cause for concern in the execution of reprocessing methods by the end-user. In a recent study conducted by Jolly, et al. (2011) 24 nursing students were asked to reprocess an endoscope as an independent task using the manufacturer's instructions. The study reported that none of the 24 participants were able to reprocess the endoscope without error [39]. As the first published usability test [39] for reprocessing reusable medical devices, it clearly makes the point that there are human factors issues related to reprocessing.

The focus of this thesis was to improve methods for validating cleaning protocols required for reprocessing. Recognizing that human factors do matter in reprocessing, an

effective method that could provide simple and high-throughput verification testing of cleaning was investigated. The colorimetric assay holds value in its ability to provide a simple “yes” or “no” detection of biofilm accumulation, while also being easy to execute. Jolly, et al. (2011) determined that one of the three reasons for the observed error in reprocessing was inconsistent or lack of feedback [39]. Participants reported that they had no way of knowing if what they were doing was correct. Essentially, there were no feedback controls in place. A potential industry application for the colorimetric assay is a system control for ensuring adequacy in cleaning by providing real time feedback. Current validation methods require intensive, expert-level methodology such as soil extraction from the device and subsequent fluorescent imaging or biochemical testing or direct testing of the soil on the device using radionuclide sampling [13]. For a central sterile supply unit reprocessing 14,000 devices, for example, this type of methodology simply is not feasible in real-time. The industry is currently calling for improved methods in detecting bioburden on reusable devices [13,14]. In this regard, a simplistic approach is what is needed to address the human factors issues that are a primary cause of improper reprocessing.

Economic Factors

As discussed in Chapter 1, the economics of reprocessing are not favorable for OEMs’ business needs. OEMs are held to high standards for producing validation testing for a process that actually results in decreased profit margins for the product due to reductions in repurchase by the end-user. The specialized equipment and materials

required for the validation testing are not capital the OEM sees as a worthwhile investment, as a result, this type of testing is typically contracted out. Contract testing can quickly become very expensive. Moreover, FDA guidelines strongly suggest destruction testing for devices with small lumens or tight interfaces to ensure adequate cleaning [14]. This is another loss of revenue for the OEM. The loss of revenue combined with the high costs associated with rigorous validation testing required for reprocessing makes medical device reprocessing an unfavorable economic business model for OEMs. Recognizing the cost associated with reprocessing for the manufacturer, this research sought to develop a cost-effective method for detecting biofilm accumulation on reusable medical devices. Providing a cost-effective method for OEMs to implement during validation testing would reduce the economic burden on OEMs and likely improve the validation data required for proving safety and effectiveness of reprocessing protocols.

The studies presented in this thesis implemented both a colorimetric assay and confocal laser scanning microscopy (CLSM) for quantifying biofilm accumulation on medical device materials. A comprehensive evaluation of the costs associated with the experimental work for both methods (as presented in Chapters 2 and 3) was conducted to provide a realistic valuation of each method. The objective of this analysis was to characterize the cost-effectiveness of both the colorimetric assay and CLSM.

Several assumptions were included in the cost analysis. 1) A confocal microscope would not be purchased as a capital expense for the CLSM method. A conservative cost estimate for a confocal microscope is on the order of $100,000. In addition to the capital cost of a confocal microscope, recurring costs for maintenance and operation would make

this an impractical purchase for an OEM (**Table 4.2**). 2) A single experiment, n, represents the analysis of eight coupons (**Table 4.4**). 3) The number of experiments conducted in one year is 50 (**Table 4.5**). This was determined by the live/dead assay. When stored according to manufacturer's instructions the live/dead assay will remain stable for on year. The total number of reactions that live/dead assay can yield is 100 and the number of reactions required by each experiment is two. For this reason, it was assumed the live/dead assay could sustain 50 experiments in one year. 4) The rinse beakers used in the CV assay were a reusable item that could sustain a maximum of 10 experiments (**Table 4.5**). 5) Price fluctuation and inflation were not considered for projected yearly costs (**Table 4.6**).

Based on the expenditures related to each method for both capital and recurring costs, a significant cost differential between these two test methods was observed. The cost per experiment for the colorimetric assay was $23.56, while the cost per experiment for CLSM was $259.31 (**Table 4.4**). The contract time for using the confocal microscope was the largest contributing cost for the CLSM analysis method, comprising 96% of the total cost experimental cost. Despite the capital expense of the microplate spectrophotometer required by the colorimetric assay, this method yielded a yearly savings in year one of 27% (**Table 4.6**). In year two, the colorimetric assay yielded a yearly savings of 96% (**Table 4.6**). It is clear that the colorimetric assay is significantly more cost effective compared to CLSM. The low cost associated with the colorimetric assay enhances its potential for an industry relevant method used for verification and validation testing required for medical device reprocessing.

Table 4.2 Capital expenditures. Capital expenditures included only a microplate spectrophotometer (Epoch™, BioTek® Instruments, Inc., Winooksi, VT) required for absorbance analysis as apart of the CV assay method. Price determined from scientific equipment distributor.

COLORIMETRIC ASSAY	
Item	**Cost**
Microplate Spectrophotometer	$8,950.00

Table 4.3 Recurring costs. Recurring costs were calculated for all items required to conduct each method. Units and bulk costs were determined from purchase orders made during experimental work. Contract time for using the confocal microscope was determined from the rates established by the Clemson Light Imaging Facility for non-student users.

COLORIMETRIC ASSAY			
Item	**Unit**	**Bulk Cost**	**Cost Per Unit**
Crystal Violet Stain	Bottle (500 mL)	$14.28	$0.03
200 µl Pipette Tips	Box-960 tips	$59.30	$5.93
Acetic Acid	2500 mL	$34.36	$0.01
Staining Reservoirs	100pk	$58.72	$0.59
Rinse Beakers	100pk	$46.41	$0.46
CLSM			
Item	**Unit**	**Bulk Cost**	**Cost Per Unit**
L/D Assay	100 reactions	$354.00	$3.54
PTFE Tape	1 roll	$3.92	$3.92
Valup	1 vial	$50.00	$2.50
Contract Time	1 hour	$125.00	$125.00

L/D: Live/Dead

Table 4.4 Total cost per experiment (n=1). The total cost per experiment was determined from the number of units required to analyze eight coupons (with an error factor) and the cost per unit (**Table 4.3**) For example, for eight coupons only 48 mL of acetic acid was required, but extra may be consumed if a spill occurred.

COLORIMETRIC ASSAY		
Item	**Units Used Per Experiment**	**Cost Per Experiment**
Crystal Violet Stain	32 mL	$0.91
200 µl Pipette Tips	1 box	$5.93
Acetic Acid	50 mL	$0.69
Staining Reservoirs	2 reservoirs	$1.17
Rinse Beakers	32 beakers	$14.85
TOTAL		**$23.56**
CLSM		
Item	**Units Used Per Experiment**	**Cost Per Experiment**
L/D Assay	2 reactions	$7.08
PTFE Tape	1/4 roll	$0.98
Valup	1/2 vial	$1.25
Contract Time	2 hours	$250.00
TOTAL		**$259.31**

Table 4.5 Total cost per year (n=50). The total cost per year for each method was calculated for the number of units of each item required to conduct 50 experiments. Only 160 rinse beakers were needed for one year because rinse beakers are a reusable item. It was determined that if the beakers were properly cleaned and maintained between each experiment they could be used for a maximum of 10 experiments.

COLORIMETRIC ASSAY				
Item	**Units Used Per Experiment**	**Cost Per Unit**	**Units Needed for 1 Year**	**Cost Per Year**
Crystal Violet Stain	32 mL	$0.03	1,600 mL	$45.68
200 µl Pipette Tips	1 box	$5.93	50 boxes	$296.50
Acetic Acid	50 mL	$0.01	2,500 mL	$34.36
Staining Reservoirs	2 reservoirs	$0.59	100 reservoirs	$58.72
Rinse Beakers	32 beakers	$0.46	160 beakers	$74.26
TOTAL				**$509.52**
CLSM				
Item	**Units Used Per Experiment**	**Cost Per Unit**	**Units Needed for 1 Year**	**Cost Per Year**
L/D Assay	2 reactions	$3.54	100 reactions	$354.00
PTFE Tape	1/4 roll	$3.92	12.5 rolls	$49.00
Valup	1/2 vial	$2.50	25 vials	$62.50
Contract Time	2 hours	$125.00	100 hours	$12,500.00
TOTAL				**$12,965.50**

Table 4.6 Projected yearly savings. Percent savings was calculated for year one, which included the capital expenditures. It was assumed all capital expenditures would be paid in year one and would not carry over into year two. It was also assumed that all yearly expenses thereafter would be constant, as price fluctuation and inflation were not considered.

Method	Year 1	Year 2
COLORIMETRIC ASSAY	$9,459.52	$509.52
CLSM	$12,965.50	$12,965.50
Percent Savings (%)	**27.0**	**96.1**

4.4 CONCLUSION

The broad objective of this chapter was to demonstrate both the engineering and commercial significance of the research work presented in this thesis. From an engineering perspective, reprocessing of reusable medical devices is a complex process that requires careful consideration of device design. Device geometry, fluid flow principles, and material selection and surface characteristics are all engineering factors that can have a significant impact on biofilm accumulation and, subsequently, effective device reprocessing. From a commercial perspective, human factors and cost matter in medical device reprocessing. In order to sustain quality control in reprocessing of medical devices it is critical for reprocessing methods to not only be repeatable and reproducible, but to be easily monitored and traceable. The unique economic model of medical device reprocessing places a financial burden on OEMs. For this reason, a cost-efficient method for validation testing for cleaning methods is necessary for improving reprocessing outcomes.

Safe and effective reprocessing is a result of many contributing factors: device design, improved verification and validation methods for cleaning, IFUs that consider human factors, and cost. In an effort to improve the engineering and commercial considerations related to reprocessing, this work delivered a simple, cost-efficient method suitable for detecting biofilms on complex reusable medical devices in a high-throughput industry setting for the purpose of validating cleaning methods required for reprocessing

CHAPTER FIVE

CONCLUSION

Challenges associated with improper reprocessing are related to the complexity of reusable medical device design, validation of cleaning protocols required by the FDA, as well as human and economic factors. The broad objective of this thesis was to deliver a simple, cost-efficient method suitable for detecting biofilms on complex reusable medical devices in a high-throughput industry setting for the purpose of validating cleaning methods required for reprocessing.

Current methods for detecting biofilm accumulation on medical devices are established; however, these methods lack appropriate consideration for the complex design features of reusable medical devices. A colorimetric assay widely used for quantifying biofilm accumulation is suitable for the complexity of reusable medical devices; however, its application has been limited to biofilms grown in a tissue culture plate, which does not accurately represent the true growth conditions of biofilm. Modifications of this colorimetric assay were necessary to appropriately stain biofilm grown on large surface areas. Experimental work confirmed a 6 mL volume of acetic acid and a 570 nm excitation wavelength together provided a highly sensitive detection method for biofilms stained with CV. The high sensitivity of this colorimetric assay makes it ideal for detecting biofilm on reusable medical devices with complex design features.

A current, standard method for detecting biofilm accumulation, CLSM, can provide accurate quantitative data through imaging processing techniques. Experimental

work demonstrated that pixilation intensities of biofilm with fluorescent staining can be quantified using image-processing software, such as Image J. Comparing intensity ratios and absorbance measurements from the colorimetric assay for a given biofilm could demonstrate a direct relationship between the two detection modalities effectively validating the modified colorimetric assay as a method for detecting biofilm accumulation on reusable medical devices.

Once validated, the modified colorimetric assay has potential for becoming an industry relevant method for improving medical device reprocessing outcomes. The industry is currently calling for improved methods in detecting bioburden on reusable devices. The colorimetric assay provides highly sensitivity detection of biofilm and is applicable to devices with complex designs. Additionally, it is a simplistic approach to validating cleaning protocols required by the FDA, which is what is needed to address the human factors issues that are a primary cause of improper reprocessing. Finally, the modified colorimetric assay improves the financial burden incurred by OEMs by providing yearly cost savings of 96% when used as a validation method instead of conventional confocal microscopy. Reducing costs associated with reprocessing creates an incentive for OEMs to improve device designs for reprocessing and produce feasible reprocessing protocols that can be adequately executed in an industrial system.

In conclusion, this thesis presents a modified colorimetric assay for detecting biofilm accumulation on reusable medical devices that offers an innovative solution to the current challenges associated with medical device reprocessing.

APPENDICES

APPENDIX A

RAW DATA FOR STATISTICAL ANALYSIS

Table A.1 Absorbance data and contributing effects variables. Data were analyzed using a generalized linear model and a binomial distribution to test for the effects of material, inoculum concentration, flow conditions, channel position, wavelength, and acetic acid volume on absorbance.

Run	Material	Innoculum Concentration [Log_{10}CFU/mL]	Flow/Channel	Acetic Acid Volume[mL]	Absorbance 492 nm	Absorbance 570 nm
1	SS	10.3	3	20	0.069	
1	SS	10.3	5	20	0.547	
2	SS	9.9	2	20	0.173	
2	SS	9.9	5	20	0.351	
3	SS	5.3	4	20	0.215	
3	SS	5.3	5	20	0.415	
4	SS	9.7	1	20	0.135	
4	SS	9.7	5	20	0.519	
5	SS	9.1	3	20	0.204	
5	SS	9.1	5	20	0.136	
4	SS	9.7	1	20		0.717
4	SS	9.7	5	20		3.454
5	SS	9.1	3	20		1.469
5	SS	9.1	5	20		0.998
1	PC	10.3	2	20	0.091	
1	PC	10.3	5	20	0.114	
2	PC	9.9	1	20	0.145	
2	PC	9.9	5	20	0.134	
3	PC	5.3	3	20	0.179	
3	PC	5.3	5	20	0.095	
4	PC	9.7	4	20	0.055	
4	PC	9.7	5	20	0.551	
5	PC	9.1	2	20	0.048	
5	PC	9.1	5	20	0.129	
4	PC	9.7	4	20		0.137
4	PC	9.7	5	20		3.52
5	PC	9.1	2	20		0.124
5	PC	9.1	5	20		0.823
2	PP	10.3	5	20	0.157	
2	PP	9.9	4	20	0.151	
2	PP	9.9	5	20	0.344	
3	PP	5.3	2	20	0.211	
3	PP	5.3	5	20	0.064	
4	PP	9.7	3	20	0.263	
4	PP	9.7	5	20	0.375	
5	PP	9.1	1	20	0.185	

5	PP	9.1	5	20	0.175	
4	PP	9.7	3	20		1.668
4	PP	9.7	5	20		2.634
5	PP	9.1	1	20		1.718
5	PP	9.1	5	20		1.508
1	SI	10.3	4	20	0.197	
1	SI	10.3	5	20	0.453	
2	SI	9.9	3	20	0.316	
2	SI	9.9	5	20	0.167	
3	SI	5.3	1	20	0.459	
3	SI	5.3	5	20	0.064	
4	SI	9.7	2	20	0.191	
4	SI	9.7	5	20	0.107	
5	SI	9.1	4	20	0.05	
5	SI	9.1	5	20	0.075	
4	SI	9.7	2	20		1.086
4	SI	9.7	5	20		0.528
5	SI	9.1	4	20		1.469
5	SI	9.1	5	20		0.375
6	SS	9.4	2	6	0.583	
6	SS	9.4	5	6	0.445	
7	SS	5.4	4	6	0.307	
7	SS	5.4	5	6	2.375	
6	PC	9.4	1	6	0.187	
6	PC	9.4	5	6	0.234	
7	PC	5.4	3	6	0.094	
7	PC	5.4	5	6	0.849	
6	PP	9.4	4	6	0.275	
6	PP	9.4	5	6	0.374	
7	PP	5.4	2	6	0.120	
7	PP	5.4	5	6	1.134	
6	SI	9.4	3	6	0.156	
6	SI	9.4	5	6	0.111	
7	SI	5.4	1	6	0.065	
7	SI	5.4	5	6	0.107	
6	SS	9.4	2	6		3.650
6	SS	9.4	5	6		3.466
7	SS	5.4	4	6		2.721
7	SS	5.4	5	6		3.987

6	PC	9.4	1	6		1.306
6	PC	9.4	5	6		2.225
7	PC	5.4	3	6		0.484
7	PC	5.4	5	6		3.646
6	PP	9.4	4	6		1.962
6	PP	9.4	5	6		3.355
7	PP	5.4	2	6		0.895
7	PP	5.4	5	6		3.702
6	SI	9.4	3	6		0.878
6	SI	9.4	5	6		0.800
7	SI	5.4	1	6		0.275
7	SI	5.4	5	6		0.725

APPENDIX B

GROSS PHOTOS OF EXPERIMENTAL SET-UP

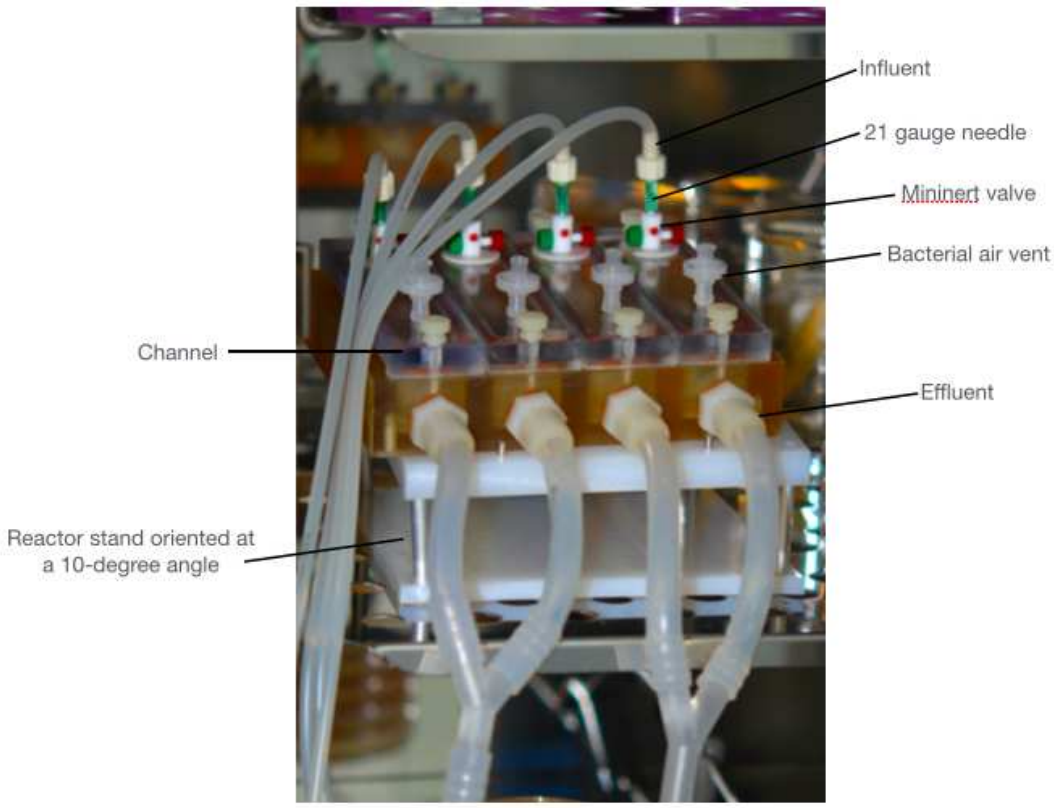

Figure B.1 Drip flow reactor set-up inside incubator. Flow of TSB is delivered in silicone tubing to each channel through the influent mininert valve and 21-gauge needle. Reactor is positioned at a 10-degree angle, which provides gravitational fluid flow over coupon inside each channel. Waste is removed via effluent ports into a waste carboy (not pictured).

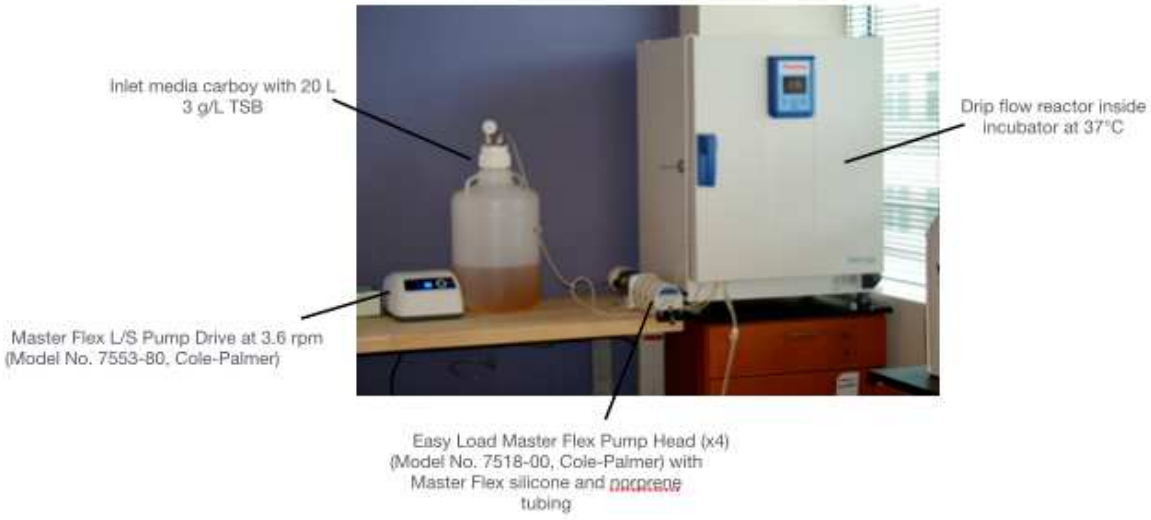

Figure B.2 Laboratory set-up of peristaltic pump system and drip flow reactor. Peristaltic pump system delivers flows of 3 g/L TSB media from inlet media carboy to reactor at a flow rate of 0.92 mL/min/channel. Reactor is inside incubator at 37°C.

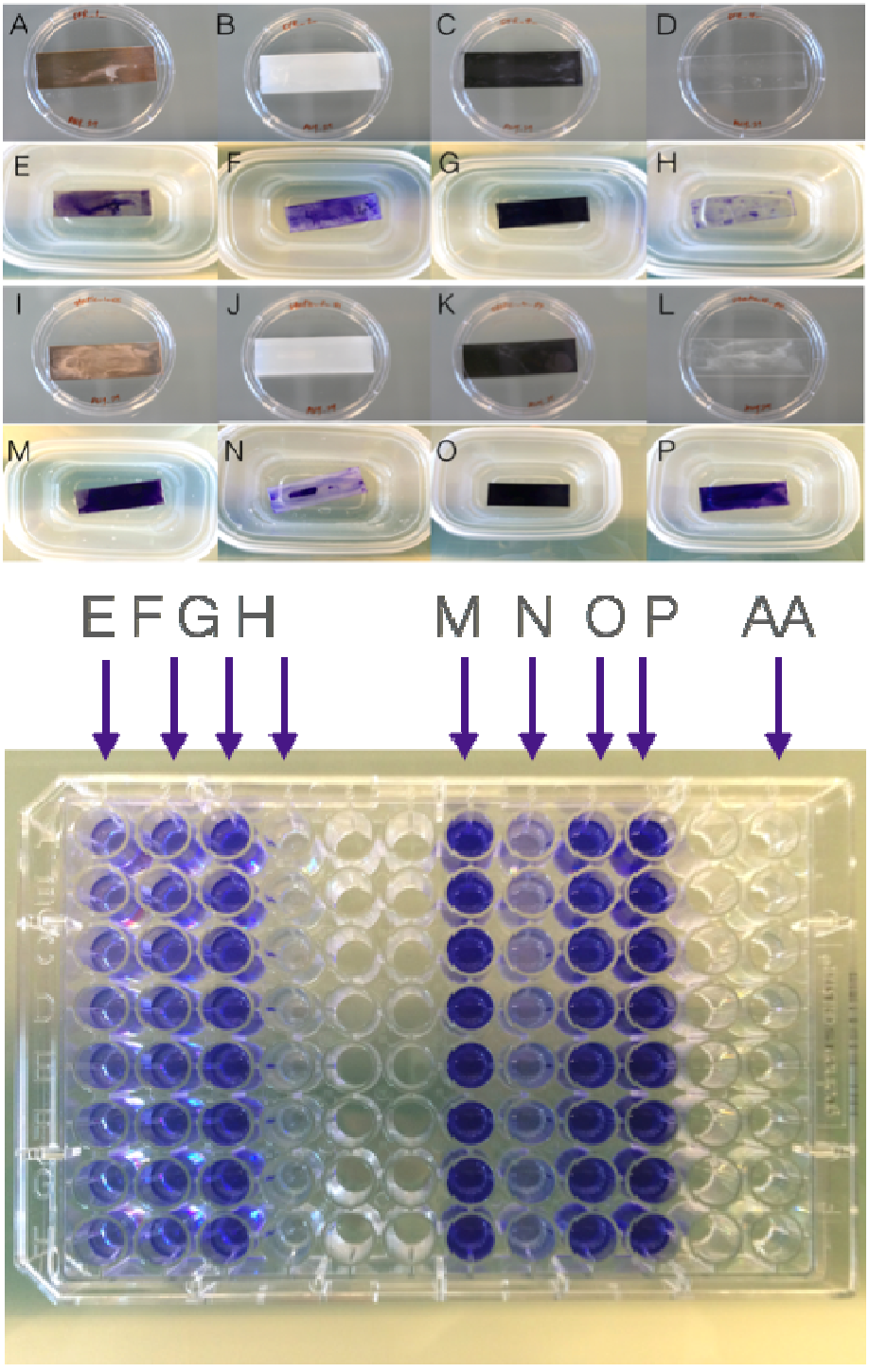

AA: acetic acid

Figure B.3 Illustration of CV staining on coupons and corresponding CV solutions in a 96- well plate. (A-D): Biofilms grown in DFR, **(E-H):** DFR biofilms stained with crystal violet, **(I-L):** Biofilms grown statically, **(M-P):** Static biofilms stained with crystal violet. 96-well plate loaded with eluted crystal violet from coupons pictures.

REFERENCES

1. Reprocessed Medical Devices Market- Global Industry Analysis, Size, Share, Growth, Trends, and Forecast, 2014-2020. (2014). Transparency Market Research. (Web). http://globenewswire.com/news-release/2014/09/17/666582/10098979/en/Reprocessed-Medical-Devices-Market-Expected-to-Reach-USD-2-58-Billion-Globally-in-2020-Transparency-Market-Research.html

2. Vukelich, D.J. (2012). Association of Medical Device Reprocessors Celebrates 15 Years of Cutting Healthcare Spending. Association of Medical Device Reprocessors. (Web). http://www.amdr.org/tag/ethicon-endo-surgery/

3. Association of Medical Device Reprocessors (2011). The Business Case for Reprocessing. (Web). www.amdr.org/wp.../04/Business-Case-for-Reprocessing-for-web.pdf

4. U.S. Food and Drug Administration. (2014). Reprocessing of Reusable Medical Devices. (Web). http://www.fda.gov/MedicalDevices/DeviceRegulationandGuidance/ReprocessingofReusableMedicalDevices/default.htm

5. Rutala, W.A et.al. (2008). Guideline for Disinfection and Sterilization in Healthcare Facilities. The Center for Disease Control and Prevention.

6. Donlan, R.M. (2002). Biofilms: Microbial Life on Surfaces. Emerg Infect Dis. doi:10.3201/eid0809.020063

7. Dancer, S.J, et.al (2012). Surgical Site Infections Linked to Contaminated Surgical Instruments. J Hospital Infection. 81:231-238

8. Pinto, F.M.G, et.al (2010). Analysis of Microbial Load in Instruments Used in Orthopedic Surgeries. Am J Infect Control. 38:229-233

9. John, J.F, Davidson, R.J, Low, D.E (2012). *Staphylococcus epidermidis* and Other Coagulase-Negative *Staphylococci.* Antimicrobe. (Web). http://www.antimicrobe.org/new/b234.asp

10. Roberts, C.G. (2013). The Role of Biofilms in Reprocessing Medical Devices. Am J Infect Control 41:S77-S80

11. Tosh, P.K, et.al (2011). Outbreak of *Pseudomonas aeruginosa* Surgical Site Infections After Arthroscopic Procedures: Texas, 2009. Infection Control and Hospital Epidemiology. 32:12

12. FDA. (2004). Summary of the Medical Device User Fee and Modernization Act of 2002.

13. Vockley, M. (2011). Priority Issues from the AMMI/FDA Medical Device Reprocessing Summit. The Association for the Advancement of Medical Instrumentation.

14. U.S. Food and Drug Administration. (2011). Draft Guidance for Industry and FDA Staff. Processing/Reprocessing Medical Devices in Health Care Settings: Validation Methods and Labeling.

15. Donlan, R.M. (2001). Biofilm Formation: A Clinically Relevant Microbiological Process. Clinical Infectious Diseases, 33,1387-92.

16. Maki, D, et.al (1977). A Semiquantitative Culture Method for Identifying Intravenous-Catheter Related Infection. N Engl J Med, 296:1305-1309

17. Kite, P, et.al (1997). Evaluation of a Novel Endoluminal Brush Method for in-situ Diagnosis of Catheter Related Sepis. J Clin Pathol, 50:278-282

18. Donlan, R.M, et.al (2001). Protocol for Detection of Biofilms on Needleless Connectors Attached to Central Venous Catheters. J Clin Microbiol, 39(2):750

19. Zelver, N, et.al (2001). Development of a Standardized Antibiofilm Test. Methods in Enzymology, 337:363-376

20. Joyce, E, et.al (2003). The Development and Evaluation of Ultrasound for the Treatment of Bacterial Suspensions. A Study of Frequency, Power, and Sonication Time on Cultured *Bacillus* Species. Ultrasonics Sonochemistry, 10(6):315-318

21. Christensen, G, et.al (1985). Adherence of Coagulase-Negative Staphyloccoci to Plastic Tissue Culture Plates: a quantitative model for the adherence of staphylococci to medical devices. J Clin Microbiol, 22(6):996

22. Rudolph, K. (2012). Course Lecture Material. General Microbiology. Clemson University, Clemson, SC.

23. Buckingham-Meyer, K, et.al (2007). Comparative Evaluation of Biofilm Disinfectant Efficacy Tests. J Microbial Methods, 70(2):236-244

24. Kwansy, S, et.al (2010). Static Biofilm Cultures of Gram-Positive Pathogens Grown in Microtiter Format Used for Anti-Biofilm Drug Discovery. Curr Protoc Pharmacol. 50:13A.8.1-13A.8.23

25. Pereira, M, et.al (2002). Effect of Flow Regime on the Architecture of a *Pseudomonas fluorescens* Biofilm. J Biotechnology and Bioengineering, 78:2

26. Cunningham, A, Lennox, J, & Ross, R (2010). Biofilm Growth and Development. Biofilms: The Hypertextbook. (Web). http://www.cs.montana.edu/webworks/projects/stevesbook/contents/chapters/chapter002/section002/black/page001.html

27. Ross, S, et.al (2014). Quantification of Confocal Images of Biofilms Grown on Irregular Surfaces. J Microbial Methods. 100:111-120

28. Jefferson, K, et.al (2005). Use of Confocal Microscopy to Analyze the Rate of Vancomyocin Penetration through *Staphylococcus aureus* Biofilms. American Society for Microbiology. 49(6):2467

29. Kuehn, M, et.al (1998). Automated Confocal Laser Scanning Microscopy and Semiautomated Image Processing for Analysis of Biofilms. Appl Environ Microbiol. 64(11):4115

30. An, Y.H, & Friedman, R.J. (1997) Laboratory Methods for Bacterial Adhesion. J Microbial Methods. 30:141-152

31. Wu, Y, et.al (2011). Differential Response of *Staphylococci* and Osteoblasts on Varying Titanium Surface Roughness. J Biomaterials. 32:4(951-960)

32. Mcabe, W, Smith, J, & Harriott, P (2004). Unit Operations of Chemical Engineering. (7^{th} ed.). (pp.114-117). McGraw-Hill

33. Manivannan, G (2008). Disinfection and Contamination: Principles, Applications and Related Issues. (pp.177-193). CRC Press, Inc.

34. Varadarajulu, S M.D, et.al. (2011). Report on Emerging Technologies. Gastrointestinal Endoscopy 74:1 doi:10.1016/j.gie.2011.01.061

35. Purevdorj, B, Costerton, J.W, & Stoodley, P (2002). Influence of Hydrodynamics and Cell Signaling on the Structure and Behavior of *Pseudomonas aeruginosa* Biofilms. Appl. Environ. Microbiol, 68(9):4457

36. Drescher, K, et.al (2012). Biofilm Streamers Cause Catastrophic Disruption of Flow with Consequences for Environmental and Medical Systems. PNAS doi:10,1073/pnas.1300321110

37. Olympus (2002). Olympus KV-5 Suction Pump. (Web). http://www.olympus.co.uk/medical/en/medical_systems/mediacentre/media_detail_7490.jsp

38. Craig, D. (2012) Titanium Surgical Instruments. Purdue University. (Web). https://www.distance.purdue.edu/training/cssp/cis/pdf/CIS228.pdf

39. Jolly, J.D, et.al, (2011). Patient Safety and Reprocessing: A Usability Test of the Endoscope Reprocessing Procedure. Human Factors and Ergonomics in Manufacturing & Service Industries doi:10.1002/hfm.20386